April 2022

Connections between Interglacial Variation and Lithological Variability within Midland Basin Permian Shale Rocks in Martin County, Texas

Helen Rice Hammon
Louisiana State University at Baton Rouge

CONNECTIONS BETWEEN INTERGLACIAL VARIATION AND LITHOLOGICAL VARIABILITY WITHIN MIDLAND BASIN PERMIAN SHALE ROCKS IN MARTIN COUNTY, TEXAS

A Thesis

Submitted to the Graduate Faculty of the
Louisiana State University and
Agricultural and Mechanical College
in partial fulfillment of the
requirements for the degree of
Masters of Geology

in

The Department of Geology and Geophysics

by
Helen Hammon
B.S., University of Texas, 2018
May 2022

ACKNOWLEDGMENTS

I would like to first express my sincere gratitude to my advisor, Dr. Peter Clift. I would not have been able to complete this thesis without his kindness, guidance, and support. I am also thankful for my committee members, Dr. Phil Bart and Dr. Guangsheng Zhuang, for their insightful advice which helped improve my research. Lastly, I would like to thank my dearest friends and family for all of their support.

TABLE OF CONTENTS

ABSTRACT

The Upper Pennsylvanian (323.2–289.9 Ma) and Lower Permian (289.9-251 Ma), (Wolfcamp and Spraberry formations) interval of the Midland Basin, West Texas, contains a mixed succession of shale, carbonate, and siltstone/sandstone lithofacies that accumulated in a deep-water marine environment under variable hydrographic restrictions. The heterogenous stratigraphy found in the Wolfcamp and Spraberry formation was formed in response to variations in sea level and a transition from a glacial to an interglacial climate during the Early Permian. These fluctuations left behind alternating beds of mudstone and carbonate, interwoven with thin sandstone beds. Because the Wolfcamp and Spraberry formations are highly heterolithic, it is critical to understand how the stratigraphic and lateral variability in lithology changes if they are to be exploited as hydrocarbon reservoirs. A highly-resolved (5-cm vertical) X-Ray fluorescence (XRF)-based chemostratigraphic study was undertaken on eleven wells from Martin Co., Texas. The study incorporates data from cuttings and cores from intervals of the Wolfcamp and Spraberry formations. Major and trace elements compositions were measured on cuttings and slabbed cores using XRF methods. Correlation of the geochemical data across the wells was undertaken in order to correlate known changes in climate with changes in lithology. After correlation of chemofacies across the eleven wells was completed, a sequence stratigraphy analysis was conducted in order to assign general basin conditions to each major sea level change.

CHAPTER 1. INTRODUCTION

Sea level changes driven by climatic cycles partly control the transport of clastic materials from continental source regions into marine sedimentary basins, with material being preferentially fluxed to the deep water during low stands and sequestered on the basin margins during high stands (Vail et al., 1977). The shelf margin stratigraphy would thus be expected to have preserved the stratigraphic responses in lithology due to base level forcing under different climatic conditions (Haq et al., 1987). In detail however the process can be complicated depending on the geometry (width and slope) of the shelf, the extent of the terrestrial drainage basin, the nature of climate onshore, as well as the tectonic state of the source terrains which help control the rate of sediment supply. Although these questions have been addressed in the recent geological past it is less clear how climatic cycles have impacted basin stratigraphy in deep time (>100 m.y.).

In this thesis I test whether the clastic material deposited under glacial and non-glacial climatic conditions cycles can be identified and mapped across a sedimentary basin in order to create greater insight into the impacts of sea level fluctuations. The Permian Basin is the ideal place to test this hypothesis because of the large amount of data that has been collected from this area and the associated research which lays the groundwork for more detailed questions to be addressed. Because of this, there is good age control on the strata in this area. The Late Pennsylvanian and Early Permian periods have been chosen because during this time there was a transition from a glacial to a non-glacial period with oscillations of regression and transgression occurring throughout each, that might be expected to have created heterogeneity in the lithologies throughout the Permian Basin (Fig. 5) (Scheffler et al., 2003).

The Permian Basin of West Texas and Southeastern New Mexico is one of the leading sources of hydrocarbons being produced in the US today. As of September 2018, the Permian Basin has produced more than 33.4 billion barrels of oil and about 118 trillion cubic feet of natural gas (EIA). Initial exploration of the Permian Basin was directed at conventional hydrocarbon plays and much of the research conducted in the basin focused on the carbonate systems (Dutton et al., 2005). The basin reached peak production in the early 1970s but after the downswing in the hydrocarbon market in the early 1980s the basin saw a steep decline in production. Because of new technologies such as hydraulic fracturing, horizontal drilling, and completion technology advancements, the Permian Basin has now surpassed the peak production rate that occurred in the 1970s (Chaudhary et al., 2011).

The newly developed technologies allow for optimization of unconventional reservoirs. Unconventional reservoirs are defined as a number of diverse systems that can only be economically beneficial after large-scale stimulation by special recovery methods (Holditch, 2003; Vidas and Hugman, 2008). Some of the most common unconventional systems include gas shale, tight gas sand, coal bed methane, and heavy oil (Chaudhary et al., 2011). In the past it was understood that these unconventional plays contained hydrocarbons, but it was not known how to extract them, so that they were thought of as sources and seals. The processes used to exploit unconventional reservoirs, hydraulic fracturing, flooding, and steam injection, allow production from mudrocks with permeability flow rates on the order of microdarcies (Cortez, 2012).

Basinal mudrocks and other associated facies of the Wolfcamp and lower Leonard formations in the Midland Basin make up the Wolfberry play, which produced 232 million barrels of oil and 592 trillion cubic feet of gas between 1998 and 2011 (Fig. 1) (Hamlin and Baumgardner, 2012). There have been a lot of publications and research on the Pennsylvanian-

Permian aged carbonate platforms and shelves of the Midland Basin, but now with the technology to access hydrocarbons in mudrocks, it is important to understand the chemistry and lithology of the basinal sediments if their full potential is to be reached. In order to fully comprehend what controls the formation and extent of these lithological layers, connections between the heterogeneous Wolfcamp and Spraberry plays need to be linked to fluctuations in sea level during the Permian.

The Wolfberry play is one of the largest oil plays in the United States. The Texas Rail Road Commission (RRC), which regulates the oil and gas production in the state, does not recognize the Wolfberry as a field or producing formation (Hamlin and Baumgardner, 2012). Instead of a recognized Wolfberry play, the RCC recognizes the Sprayberry Trend and the Wolfcamp Formation. The Spraberry Formation was classified in 2009 as the second-largest oil field in the United States. The Spraberry Trend data capture about 88% of the Wolfberry production with the remained 12% assigned to other field names (Hamlin and Baumgardner, 2012).

Sandstone reservoirs found in the Wolfberry play mainly occur in the Spraberry and Dean formations (Fig. 1). Because porosity and permeability in the northern half of the basin is better, reservoir quality is superior to that in the southern Midland Basin, but producing areas are still small (Hamlin and Baumgardner, 2012). The best reservoirs in the Wolfcamp Formation and Leonardian Formation are found in the slope and basin facies carbonate reservoirs that were developed near the platform margins (Dutton et al., 2005). Therefore, the basinal deposits create isolated reservoirs, of good quality enclosed in broad areas with only marginal reservoir quality (Hamlin and Baumgardner, 2012).

The basinal deposits in the Midland Basin are highly heterolithic and therefore it is extremely difficult to predict the stratigraphic and lateral variability in lithologic changes (Hammon et al., 2019). The ability to map the lithologic heterogeneity of the Wolfcamp and Leonard formations would help in understanding the evolution of hydrocarbons and how to best extract them, as well as more broadly to understand how climatic cycles impact the stratigraphy of sedimentary basins. The purpose of this study is to use core and cutting-derived data together with wireline logs to define and describe the basinal facies of the Wolfcamp and lower Leonard intervals in Martin County, Texas and correlate these chemostratigraphic units with sea level change.

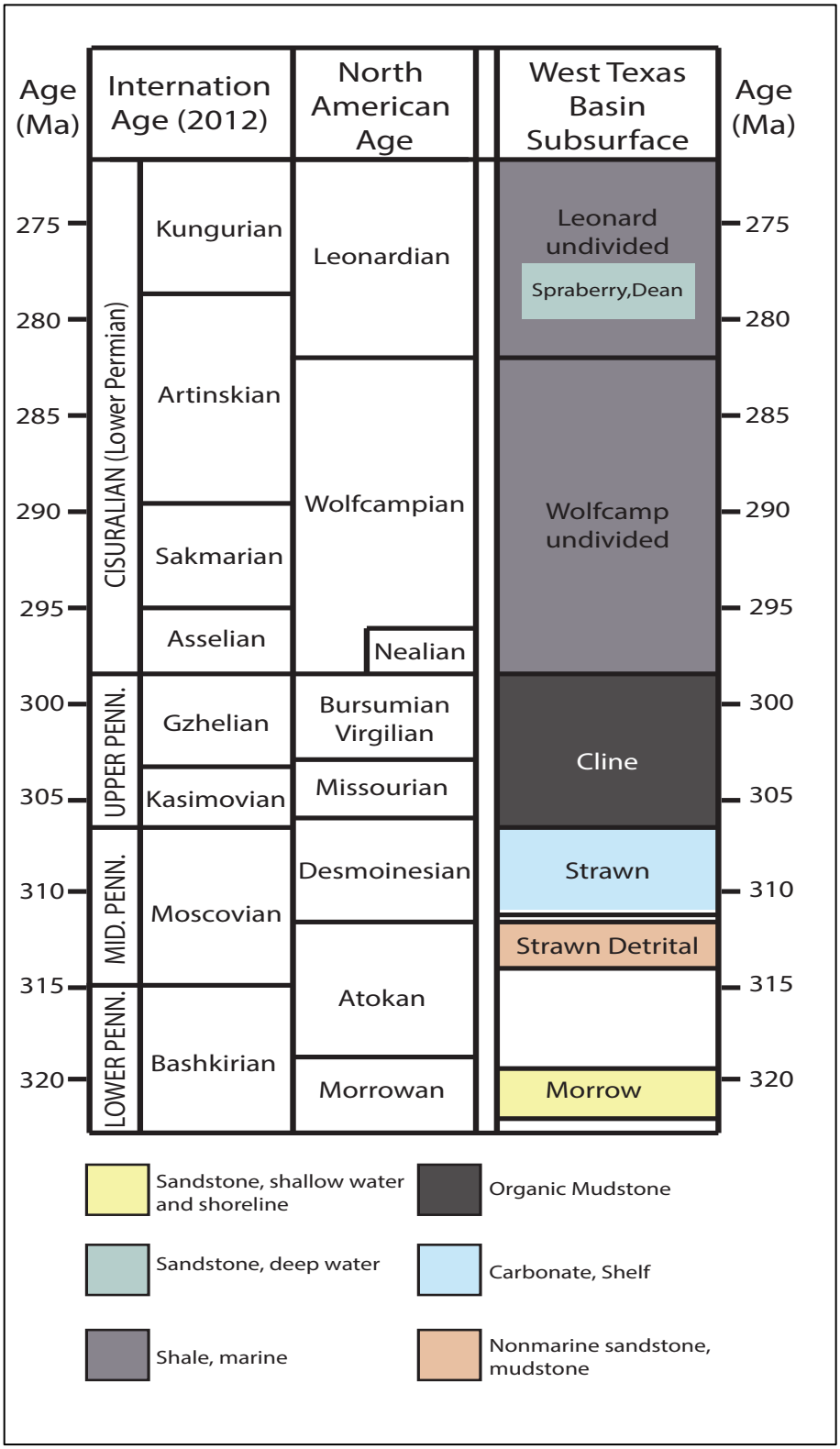

Figure 1. Stratigraphy of the subsurface of West Texas basins, including the Midland and Delaware basins during the Pennsylvanian and Permian time. Adapted from Ewing (2016).

1.1. Study Area

Martin County is located in West Texas just north of Midland. It lies within the Midland Basin which is the eastern subbasin of the Permian Basin. Martin County is about 916 square miles in area. This region lies southeast of the Horseshoe Atoll and is wedged between the Central Basin Platform and the Eastern Shelf (Fig. 2). The northwest corner of Martin County barely touches the edge of the Horseshoe Atoll.

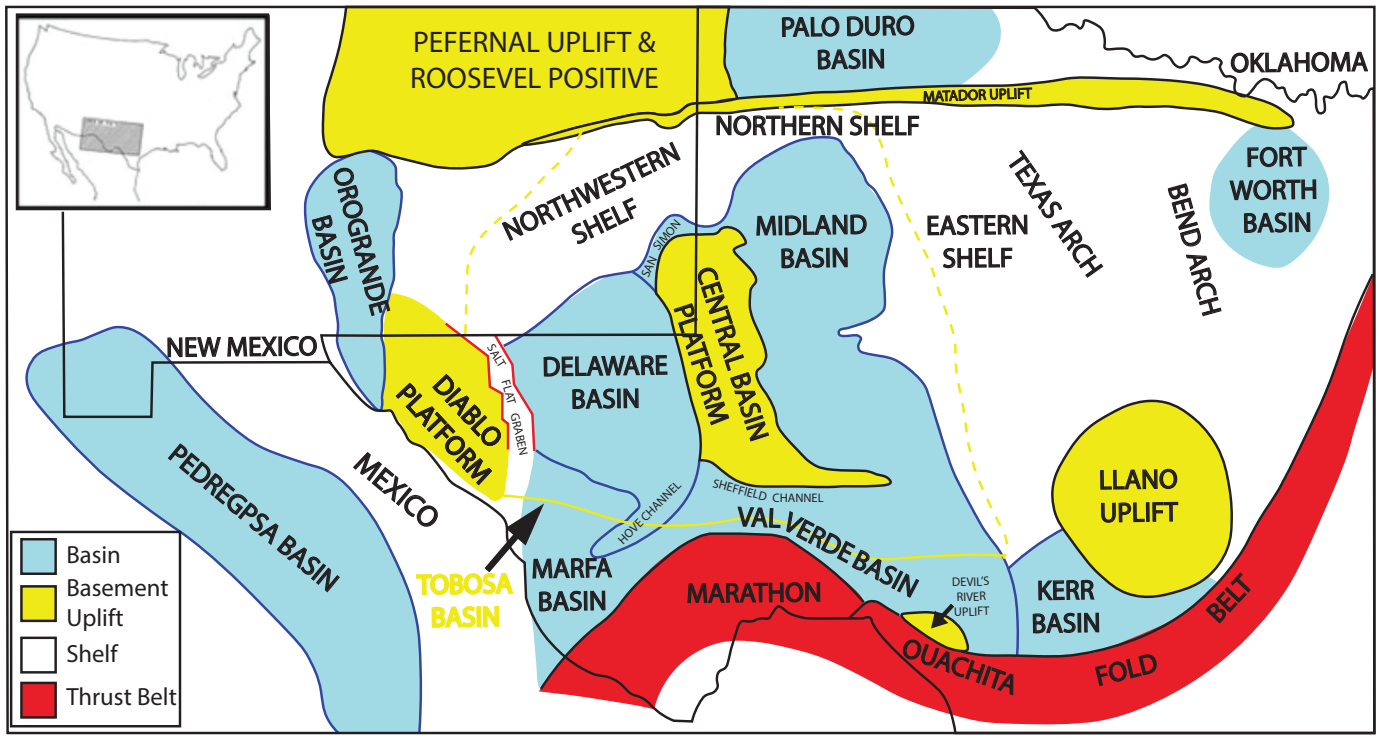

Figure 2. Map of major basins and uplifts found in West Texas

CHAPTER 2. BACKGROUND

2.1. Geologic Setting

The Midland Basin is a subbasin in the eastern portion of the Permian Basin of West Texas and southeastern New Mexico. This deep-water basin is surrounded by three pre-Permian carbonate platforms. These platforms include the Central Basin Platform, the Northern Shelf, and the Eastern Shelf and these began to form during the opening of the Paleozoic Tobosa Basin during the Early Permian (Frenzel et al., 1988; Hamlin, 2009) (Fig. 2).

Before the uplift of the Central Basin Platform that occurred during the Pennsylvanian, the area consisted of low relief features within one basin, the Paleozoic-aged Tobosa Basin (Bhatnagar et al., 2019; Hoak et al., 1998). During the mid-late Pennsylvanian basement rocks were uplifted, splitting the Tobosa Basin into the Delaware Basin to the west and the Midland Basin to the east, with the Central Basin Platform dividing the two in the middle. The Central Basin Platform's basement was uplifted in the mid-to late Pennsylvanian and then capped with a carbonate reef during the Wolfcamp (Fig. 2). As uplift of the Central Basin Platform was occurring the Midland and Delaware Basins began to subside (Frenzel et al., 1988; Hoak et al., 1998; Yang and Dorobek, 1995).

During the Pennsylvanian Texas and the Permian Basin were subequatorial and had a shallow-water environment, allowing for the formation of carbonate platforms that covered most of the basin (Ewing et al., 2016; Peng et al., 2021). These carbonate reefs were deposited on top of the flat erosional unconformity created after the uplift of the Central Basin Platform (Hoak et al., 1998; Zhang and Slatt, 2019). After the mid-late Pennsylvanian, these carbonate platforms broken apart because of faster subsidence in the basinal areas. As a result of the subsidence, carbonate shoals formed around the central axis of the basin, especially on the east side of the

Central Basin Platform facing the Midland Basin, which created the Central Basin Platform (Ewing et al., 2016; Kvale et al., 2020). As the Central Basin Platform grew larger, the Midland Basin began to infill with 2,000 ft (610 m) of mixed organic-rich shale, limestone eroded from the Central Basin Platform and sandstone creating the Wolfcamp Formation. The last phase of uplift and faulting occurred during the Wolfcampian (299-284 Ma), and the final configuration of the deep-water subbasins of the Permian Basin were formed (Ewing et al., 2016; Green et al., 2020).

2.2. Tectonics

As the Early Permian began the Permian Basin lay on the southern margin of the North American Craton (Cortez, 2012). Gondwana was moving into its final position to create Pangea making southern North America a land-locked equatorial desert (Ewing et al., 2016; Nicot et al., 2020). While Gondwana was moving in the late Paleozoic, the South American Margin moved towards the northwest (Fig. 3)(Torsvik and Cocks, 2013). As this plate was moving, the oceanic floor deposits and overlying turbidite fan deposits that lay between North and South America became one part of a large accretionary prism of semi-consolidated sediments (Cawood and Buchan, 2007; Lawton et al., 2021; Ross, 1986). The sedimentary wedges were folded and thrusted onto the southern margin of North America. As the accretionary wedges were imbricated on top of one another, they formed highlands which eroded very rapidly. The loading of these highlands created a sequence of elongated, deep-water, depositional troughs north and west of the wedges, which infilled with thick accumulations of turbidites (Ross, 1986).

The loading by the accretionary wedges renewed faulting along northwest-north trending Precambrian zones of structural weakness. The younger, Paleozoic faults had high angle to

vertical fault planes and large horizontal displacement (Ross, 1986; Verma and Scipione, 2020). This fault system outlines the major uplifts and depocenters in the Permian Basin. Tectonism was most intense during the Early Pennsylvanian, but continued into the Early Permian (Fig. 4) (Ross, 1986). During this time of tectonism, many asymmetric anticlines were formed and faulted (Frenzel et al., 1988). Once Gondwana and Laurasia combined, during the mid-Wolfcampian, the Marathon orogenic belt was completed and the Permian Basin became a stable tectonic area (Cawood and Buchan, 2007; Yang and Dorobek, 1995). Subsequently, the tectonic uplifts became carbonate depositional platforms during the Leonardian Epoch (284-271 Ma) (Baumgardner et al., 2016).

Once the uplift of the Central Basin Platform was complete, an erosional unconformity formed, allowing the Wolfcampian carbonate structures to be deposited on a flat surface. Because of the erosional event that caused the unconformity, the underlying accretionary wedge structures, are capped by a flat carbonate, creating a complex system reservoirs and traps for subsurface liquids and gases (Baldwin, 2016; Hoak et al., 1998).

The Permian Basin began to subside as the Central Basin Platform was uplifted in the mid-late Pennsylvanian. As the subsidence of the Midland Basin occurred during the Pennsylvanian, two different arch structures formed. The Bend Arch formed to the east and separated the Midland Basin from the Fort Worth Basin, while the Matador-Red River Arch formed to the north, separating the Palo Duro Basin from the Permian Basin (Fig. 2) (Frenzel et al., 1988; Hamlin, 2009). The subsidence rates during deposition of the Strawn Formation exceeded the ability of the carbonate platform to grow. The indicative deep-water basins of the Permian Basin began to develop and submerging the Strawn carbonate platform, reaching as far as the Palo Duro Basin (Fig. 2) (Ewing et al., 2016). The subsidence continued into the

Wolfcampian and through the Permian. After the active formation of uplifts was completed, parts of the ancestral Rocky Mountains eroded into the younger sediments of the Wolfcampian. These sediments were compacted over the old, horsts (Ewing et al., 2016).

During the Wolfcampian, small amounts of tectonically driven folding and faulting occurred. The basins generally remained stable in size throughout the Wolfcampian and Leonardian. This is because the carbonate production rate kept up with the subsidence rate but was not fast enough to infill the basin. The Midland Basin was finally filled with carbonate during the Guadalupian (Cortez, 2012). Towards the end of the Wolfcampian and into the beginning of the Spraberry, the tectonics in the Permian Basin began to stabilize, as subsidence slowed.

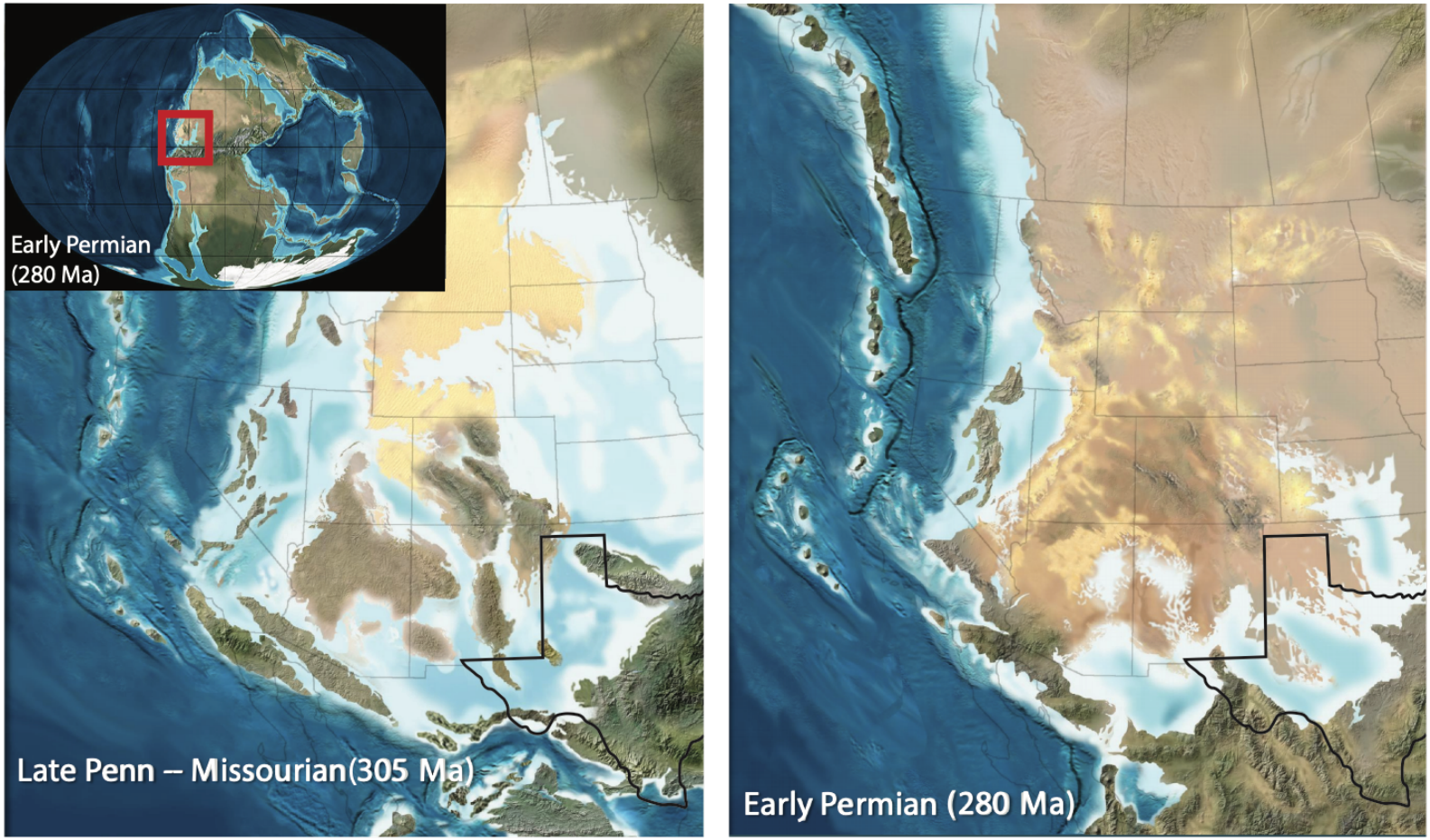

Figure 3. the movement of Gondwana into Laurasia to slowly move into their final position as Pangea. Tectonism most active during the Early Pennsylvanian. Once Gondwana and Laurasia combined in the Early Permian, the Permian Basin became a stable tectonic area. Subsidence of the basin began during Early Pennsylvanian and continued throughout the Permian (Blakey, 2013).

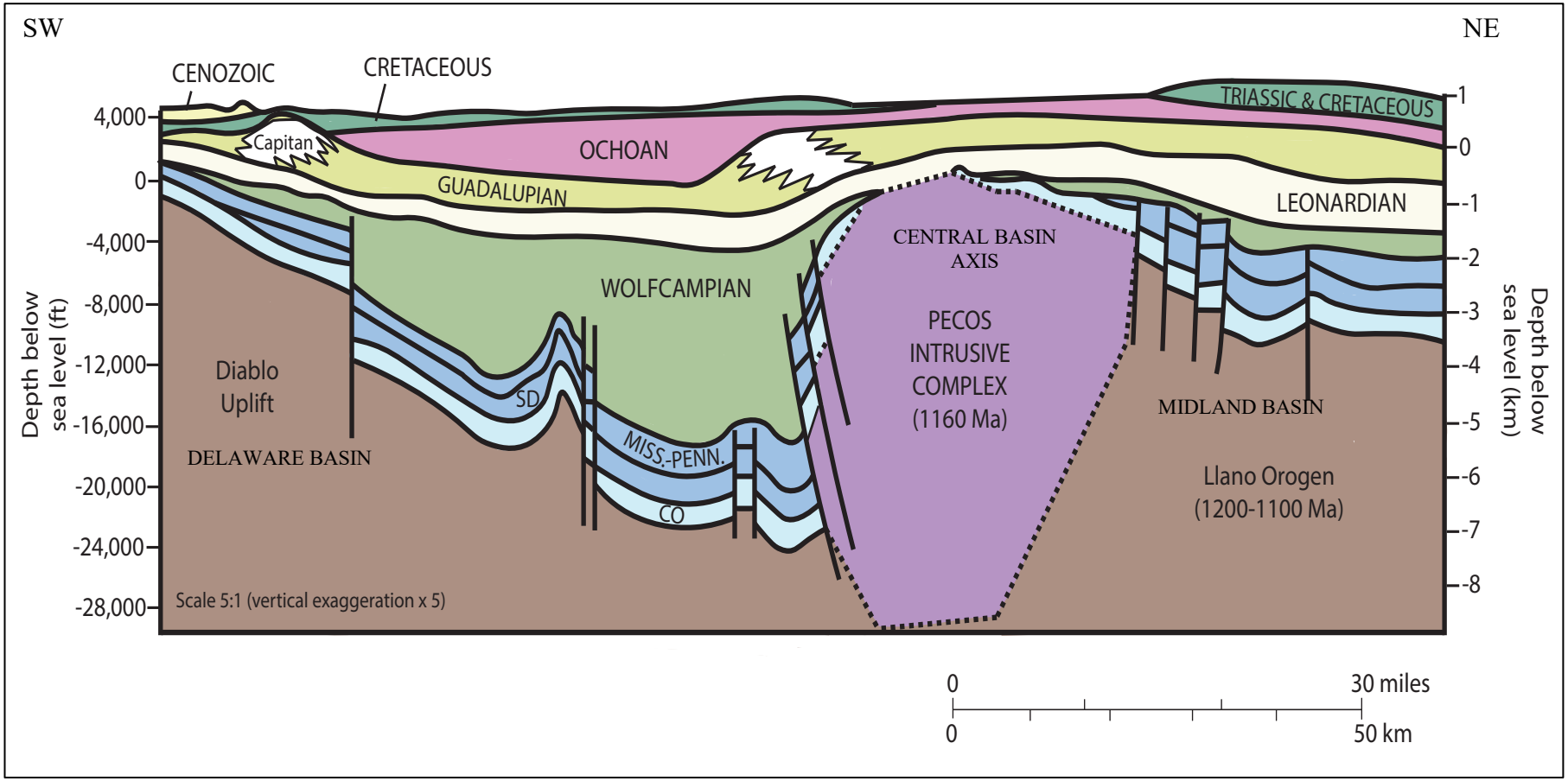

Figure 4. Crustal cross section of Permian Basin adapted from Ewing (2016). This cross section has a 5x vertical exaggeration. With the Delaware Basin located on the west side of the Central Basin Axis and the Midland Basin on the east side of the Central Basin Axis

2.3. Sea Level and Climate

The Late Pennsylvanian and Early Permian experienced an icehouse period with high amplitude and high frequency eustatic sea level fluctuations caused by repeated periods of melting and rebuilding of glaciers (Fig. 5) (Baumgardner et al., 2016). During the late Paleozoic there were short glacial events (1-8 m.y. duration) separated by times of warmer climate (Fielding et al., 2008). One of these glacial events occurred during the onset of the Permian, with the continental ice sheets at their maximum around the Asselian and Sakmarian boundary (284 Ma) (Fielding et al., 2008). The large Early Wolfcampian icesheets began to melt, driving long-term relative sea level rise (Holterhoff, 2010). Throughout the Wolfcampian, the icehouse conditions slowly reduced and North America began to experience an oscillating trend towards aridity (Baumgardner et al., 2016).

Evidence for a progressively more arid climate throughout the Wolfcamp, was found in paleosols in New Mexico and western Texas (Tabor et al., 2008). The reason for the increased aridity is that during the Early Permian Gondwana collided with Laurasia, with an 8° northward drift from the Virgilian (304-299 Ma) to Leonardian times (284-271 Ma) (Tabor et al., 2008). Once Pangea's assembly was completed, southern North America eventually became landlocked. As Gondwana moved to form Pangea, the sea level continued to fluctuate, exposing and then covering the carbonate shelves of the Midland Basin (Ewing et al., 2016; Green et al., 2020). There is also clear evidence of changes in sea level in the Midland Basin from shelf-derived allochthonous carbonates in basinal settings (Baumgardner et al., 2016).

Because of the inconsistent sea level and climate, the Midland Basin experienced many different environments throughout the Pennsylvanian and Permian. During the Pennsylvanian, the depositional environments varied from sediment-starved basins, to shallow marine carbonate

shelves, fluvial coastal plains and deltas (Frenzel et al., 1988; Hamlin, 2009; Kinley et al., 2008). During the Permian the basin also experienced a wide variety of depositional environments, but in the context of a slow transition to an arid environment. This change allowed for hypersaline, sabkha, low-energy open-marine shelves, grainstone shoals, and shelf edge organic build ups to accumulate (Frenzel et al., 1988)

There is an unconformity (Wahlman et al., 2013) which represents the product of the largest sea level drop during the deposition of the Middle Wolfcamp (292 Ma) (Candelaria et al., 1992). This major sea level fall caused the exposure and erosion of the carbonate shelves (Candelaria et al., 1992; Mazzullo et al., 1989; Wahlman et al., 2013) delivering coarse-grained carbonate debris into the basin, including large slide blocks on the eastern Central Basin Platform (Candelaria et al., 1992; Van Der Loop, 1990). After the Middle Wolfcampian unconformity, long term sea level rise continued and the carbonate shelves backstepped towards the basin margins (Wahlman et al., 2013). There is a minor unconformity, made by a sea level lowstand, that marks the end of the Wolfcampian (Wahlman et al., 2013). At this point the Leonardian began and sea level continued to rise. This transition into rapid sea level rise is marked by a Wolfcampian shale (Mazzullo and Reid, 1987). It has been estimated that throughout the early Permian, paleowater depths in the Midland Basin ranged from 500 to 2,000 ft (152 to 610 m) (Handford, 1981; Mazzullo et al., 1989).

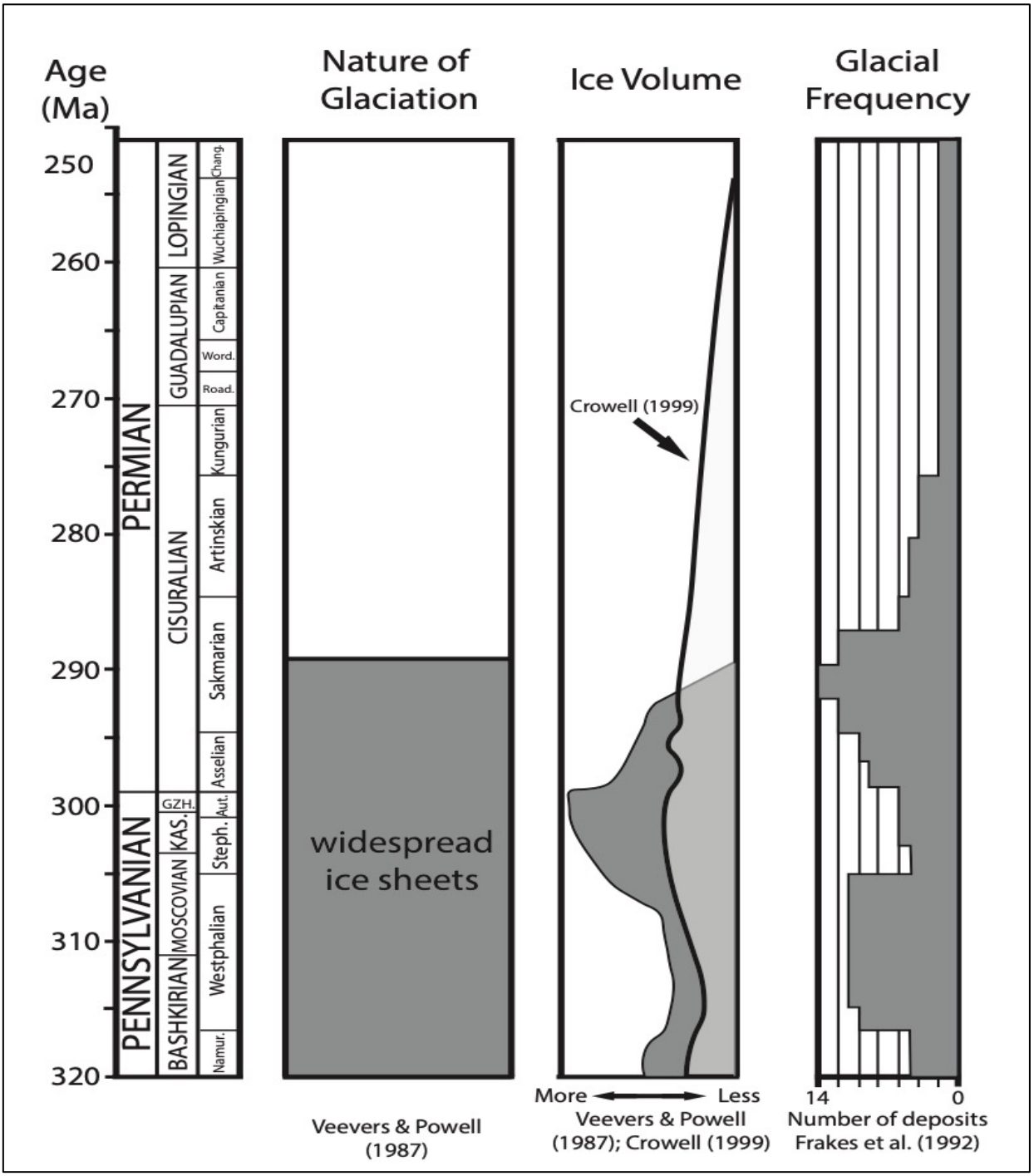

Figure 5. Stratigraphic range chart showing interpretations of the extent of glaciation through the Carboniferous and Permian Systemv(Crowell, 1999; Fielding et al., 2008; Frakes et al., 1992; Veevers and Powell, 1987).

2.4. Stratigraphy

The main lithology deposited during the Pennsylvanian was predominately gray to black marine shales with some sands, silts, gravels, and carbonates near the basin margins (Engle et al., 2016; Frenzel et al., 1988). The variety of lithologies deposited throughout the Pennsylvanian is in part a reflection of the changes in sea level and therefore, the large variety of depositional environments that existed during this time including, sediment-starved basins, shallow-marine carbonate shelves, fluvial coastal plains, and deltas (Adams et al., 1951; Frenzel et al., 1988). The sources of the sand and gravel included the Pedernal landmass in central New Mexico, high-standing Witchita-Amarillo mountains, and highlands in the Ouachita and Marathon orogens (Ewing et al., 2016). There were very few highlands and sediment sources in the direction of what is now central Texas because of the extensionally-driven subsidence that began in the Early Pennsylvanian which depressed the entire Permian Basin (Ewing et al., 2016; Green et al., 2020).

The Early to Middle Pennsylvanian rocks found in the Permian Basin are variable in distribution, thickness, and lithology due to the active tectonism that was occurring during this time. In the Midland Basin, the Pennsylvanian rocks are generally 300 m thick on the eastern and western shelves but only 150 m thick in the Central Basin (Davis, 1953; Frenzel et al., 1988; Jones and Matchus, 1984). Once the tectonism ceased and the Central Basin Platform was uplifted, an erosional unconformity made a flat erosional surface over which the strata of the Late Pennsylvanian and Early Permian could be deposited (Hoak et al., 1998).

Continuing into the Late Pennsylvanian and Early Wolfcampian, the margin was periodically clastic. During this time the margin began to prograde westward, covering the northeast Midland Basin and the eastern Horseshoe Atoll during the Late Wolfcampian (Hamlin and Baumgardner, 2012). The Permian is characterized by progradation, where carbonate shelves

from many different depositional environments advanced throughout the basin (Frenzel et al., 1988; Hemmesch et al., 2014). As the deep water margin built out to the west it deposited deep-water siliciclastic sediments (Vest Jr, 1970). The Wolfcampian strata predominantly consisted of shales with interbedded limestones and some sandstones near the basin margins (Engle et al., 2016; Frenzel et al., 1988). About 600 m of stratigraphy were deposited during the Wolfcampian in the Midland Basin and this formed horizontally bedded successions, having widespread continuity and contrasting lithologies that alternate between high and low carbonate content (Frenzel et al., 1988; Hamlin and Baumgardner, 2012; Wilde, 1976).

Focusing on the reef complexes, the Horseshoe Atoll is an isolated carbonate platform in the northern Midland Basin and this began to form in the Pennsylvanian (Sinclair et al., 2017). During the Early Permian the reef was restricted to the southwest side of the complex. At this time more than 1,100 ft (335 m) of additional limestone accumulated before the reef was buried by clastic material (Vest Jr, 1970). The other major reef complex in the Midland Basin is the Central Basin Platform. The Central Basin Platform comprises tectonically uplifted basement rock, topped with a carbonate reef.

The development of the Wolfcamp and Leonard carbonate shelves was associated with changes in sea level change. The maximum outbuilding of the Wolfcamp shelves occurred in the early to middle Wolfcampian, which was a period of rising sea levels and progradation that extended the northern shelf about 14 miles (23 km) into the basin (Mazzullo, 1995) and the eastern shelf stepped as much as 30 miles (48 km) basinward (Mazzullo et al., 1989)

Changes in sea level have been linked to the presence of shelf-derived, allochthonous carbonates in basinal settings. Allochthonous carbonates from these reef complexes were produced by processes linked with sea level fall and rise. Erosional backstepping of shelves

(Mazzullo, 1995) or an incision of a submarine canyon (Morgan et al., 1996) attributed to sea level fall could have generated the allochthonous carbonates. Also, oversteepening and collapse of seaward edges of shelf-margin carbonates attributed with sea level rise could have formed the allochthonous sediments (Mazzullo, 1995; Sivils, 2001; Sivils and Stoudt, 2001). Such processes are common during the Pleistocene under similar variable sea level conditions (Principaud et al., 2015). Sediment density flows carried these shelf-derived carbonate debris flows large distances into the Midland Basin (Baumgardner et al., 2016). The carbonate debris flow deposits extend basinward up to 25 miles (40 km) from the eastern shelf of the Central Basin Platform (Morgan et al., 1996). Packages of thin-bedded, allochthonous carbonate are found in the lower Leonard and upper Wolfcamp, extending at least 20 miles (36 km) basinward of their source located on the Central Basin Platform (Hobson et al., 1985).

The sequence formed during the Leonardian is up to 350 m thick and was deposited in deep marine waters. The Leonardian is composed of the Dean and Spraberry formations, which were deposited during times of deep water resedimentation of shelf derived carbonate debris and during times of clastic sedimentation via feeder channels and submarine canyons from the east associated with suspension settling of find grained sediment (Fig. 6) (Frenzel et al., 1988; Handford, 1981). The oldest unit found in the Leonardian is the Dean Formation, which is composed of mostly fine-grained quartzose sandstones and siltstones. The overlying formation is the Spraberry, which alternates between fine grained quartzose sandstones and siltstones, gray shales, and limestones (Frenzel et al., 1988; Wilson et al., 2020).

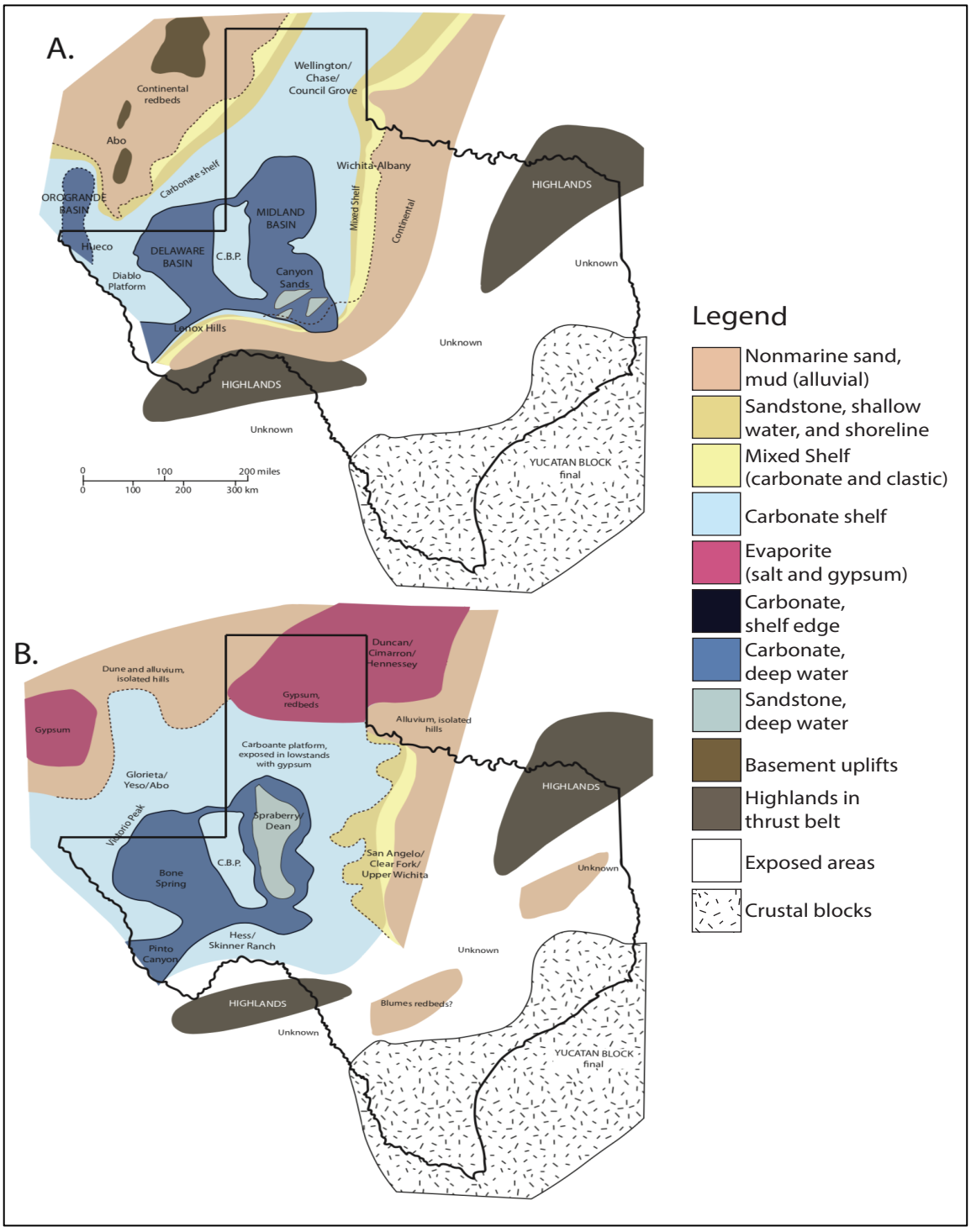

Figure 6. (A) Late Wolfcampian environments and rocks. Deep water carbonate with some deep water sandstones dominate the Midland Basin during the Wolfcamp. Adapted from Ewing (2016). (B) Leonardian highstand environments and rocks. The Spraberry and Dean formations found in the Midland basin during the Leonardian with deep water sandstones being the dominate lithofacies. Deep water carbonates are also found in the Midland basin during the Leonardian. Adapted from Ewing (2016).

2.5. Sequence Stratigraphy

Sequence Stratigraphy is the "study of rock relationships within a chronostratigraphic framework of repetitive, genetically related strata bounded by surfaces of erosion or nondeposition, or their relative conformities" (Van Wagoner et al., 1988). The principles of sequence stratigraphy state that observed stratal geometries and lithofacies distributions are the product of base level, sediment supply and production, and sediment distribution mechanisms (Vail et al., 1977). This study uses geochemical data that is correlated through eleven wells and employs the concept of sequence stratigraphy to understand the impact of the sea level fluctuations during the Late Pennsylvanian and Early Permian on the Midland Basin.

The main component of any sequence stratigraphy is the sequence, which is bounded by unconformities (i.e., sequence boundaries) and their correlative conformities. Parasequence sets and parasequences form the internal units of a sequence. A parasequence is a relatively conformable succession of genetically related beds or bedsets which are bounded by marine-flooding surfaces (Catuneanu, 2019). A parasequence set is a succession of genetically related parasequences which form a distinctive stacking pattern that is bounded, in many cases, by major flooding surfaces (Van Wagoner, 1985). There are two types of sequence boundaries. A Type 1 sequence boundary is characterized by subaerial exposure and concurrent subaerial erosion associated with stream rejuvenation, a basinward shift of facies, a downward shift in coastal onlap, and onlap of overlying strata. A Type 2 sequence boundary is distinguished by subaerial exposure and downward shift in coastal onlap landward of the depositional-shoreline break, but it lacks both subaerial erosion associated with stream rejuvenation and a basinward shift in facies (Van Wagoner et al., 1988).

Systems tracts are defined by the types of bounding surfaces, their position within the sequence and their stacking patterns. The lowstand systems tract is the lowermost systems tract that lies on top of a type on sequence boundary. The highstand systems tract is the upper systems tract in either a type 1 or type 2 sequence (Van Wagoner et al., 1988). The lateral termination of the unit is very important to understanding its significance for sea level fluctuation as well. The first type of lateral termination is “baselap” which occurs at the lower boundary of a depositional sequence. There are two distinct types of baselap, onlap and downlap. Onlap is when an initially horizontal stratum laps out against an initially inclined surface or when an inclined stratum laps out updip against a surface of greater initial inclination. Downlap is when an initially inclined stratum terminates downdip against an initially horizontal or inclined surface (Mitchum Jr et al., 1977).

Past chemostratigraphic studies linked to sequence stratigraphy in the Midland Basin suggest that Wolfcampian-Leonardian clastic sedimentary rocks were deposited under varying degrees of oxygenation (Cortez, 2012). During this time the Late Paleozoic Ice Age transitioned from a lowstand to a highstand. As a result it's possible to link the chemistry of the sediments to their location within a sequence and in turn to relate the chemistry to a time in the sealevel cycle. I use this principle when analyzing the chemistry of the drilled section and assessing the impact that sealevel changes have had on basin stratigraphy.

CHAPTER 3. OBJECTIVES AND RESEARCH QUESTIONS

3.1. Objectives

The objective of this study is to determine if changes in sea level during the Late Pennsylvanian and Early Permian can be correlated small scale changes in lithology. By evaluating and mapping the geochemical data, I should be able to identify not only changes in lithology when the climate changes from glacial to interglacial, but also identify the different sequence stratigraphy systems tracts. Understanding the impact of small-scale changes in sea level will help to further clarify the climate of the Late Pennsylvanian and Early Permian, its control over basin stratigraphy and also the development of hydrocarbons.

3.2. Research Questions and Hypotheses

-Question 1: Do changes in lithology correlate with known changes in sea level?

-*Hypothesis 1:* The Late Pennsylvanian and Early Permian were icehouse periods with smaller fluctuations in sea level due to the melting and rebuilding of ice sheets. The changes in lithology found through the Upper Pennsylvanian and Lower Permian should represent the large scale changes in sea level that occurred over this time.

-Question 2: Is there are a major shift in lithology when the climate changes from glacial to interglacial?

-*Hypothesis 2:* It is known that there was an icehouse period during the Late Pennsylvanian and Early Permian with many smaller episodes of heating and cooling (Baumgardner et al., 2016). One of the major warming events that occurred during this time is at the Pennsylvanian-Permian boundary. Following this event, the climate began to trend towards aridity. I expect to see a large

shift towards shales and carbonates after the Pennsylvanian-Permian boundary driven by reduced erosion onshore.

-Question 3: Can small changes in lithology be correlated between wells?

-*Hypothesis 3:* The Wolfcamp and Spraberry units are highly heterolithic. Some of these changes in lithology occur at an inch scale. It is unknown if these small changes in lithology are localized or seen throughout the region.

-Question 4: Can smaller oscillations of transgression and regression be predicted from changes in lithology in the deep basin?

-*Hypothesis 4:* Deposition during the Pennsylvanian and Permian, the area experienced fluctuations in sea level driven by the melting and rebuilding of glaciers. This caused repeated periods of regression and transgression. Based on the patterns found in the lithology of the Wolfcamp and Spraberry, these intervals of transgression and regression should be identifiable.

CHAPTER 4. METHODS

This study incorporates conventional slabbed cores and cuttings taken from eleven wells in Martin County, Texas (Fig. 7). All of the data come from the Lower Permian, encompassing the Wolfcamp and Spraberry units. Each well was sampled for bulk inorganic elemental geochemistry using, X-Ray fluorescence (XRF), and mineralogy using, X-Ray diffraction (XRD).

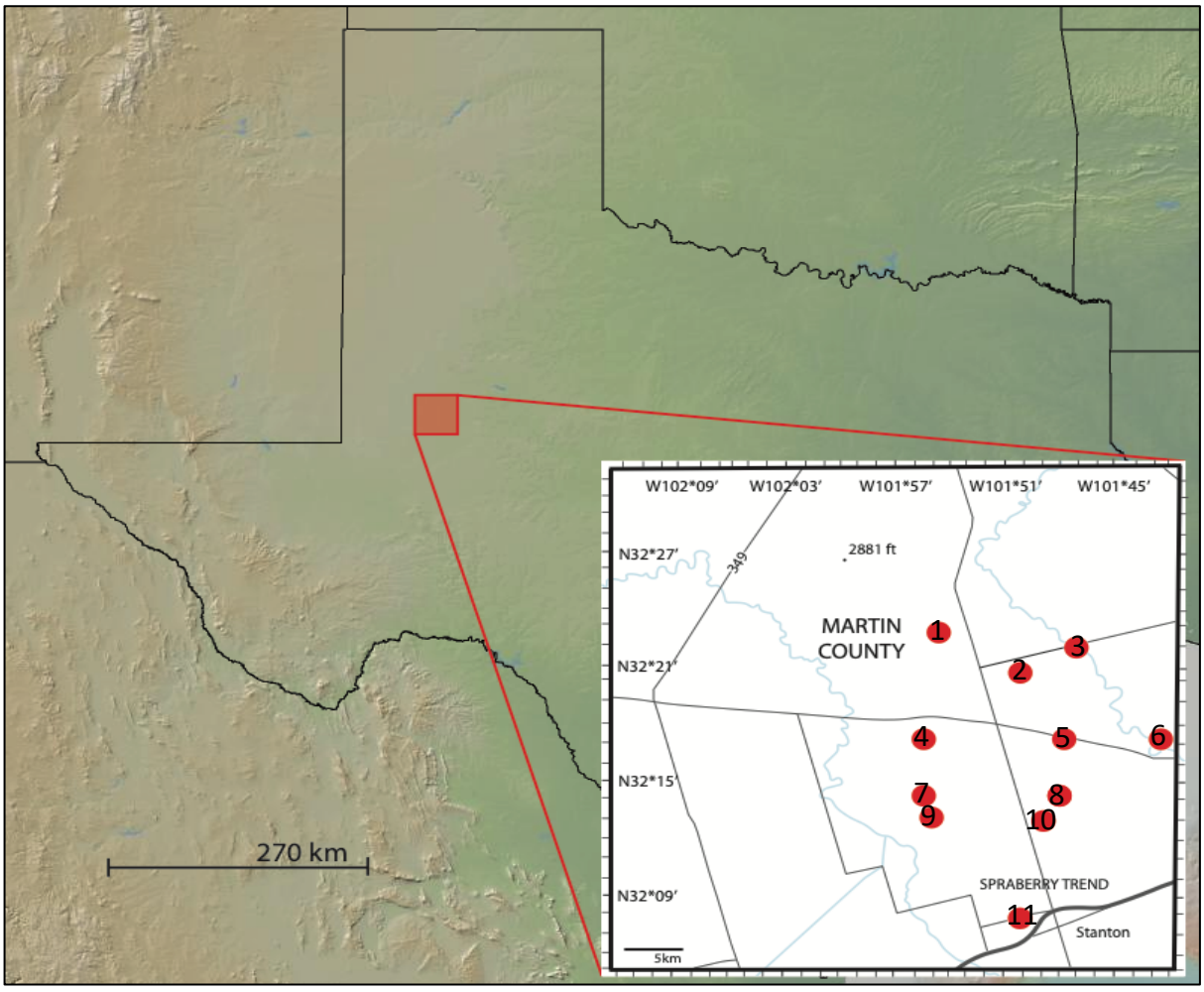

Figure 7. Topographic map of Texas with inlay of Martin County with all eleven wells in the study marked by red dots.

4.1. Geochemistry

The inorganic elemental geochemistry was measured using a Bruker Tracer IV spectrometer, following the methodology refined at the University of Texas at Arlington and the Texas Bureau of Economic Geology (Rowe et al., 2012; Rowe et al., 2017). Concerning the data collected from cores, the XRF measurements were taken on a cleaned face of a slabbed core every 2 inches (~5 cm). Conventional XRF data was also collected from cuttings. This involved the cuttings being cleaned, followed by them being pressed into pellets and then measured by XRF. The Bruker Tracer IV records photon counts that are converted into elemental abundances using a set of mudrock reference materials. The proprietary calibration consists of various shale and limestone pellets from both international standards and other common mudrock formations. Abundances from 29 different elements were collected using two different instrument settings. Major and trace elements (Al, Ca, Fe, K, Mg, Mn, Na, P, S, Si, Ti, Ba, V, Cr) were measured at 15 kV and 35 μA under a helium flow system with a 60 second count time. Trace elements (As, Co, Cu, Ga, Mo, Nb, Ni, Pb, Rb, Sr, Th, U, Y, Zn, and Xr) were collected at 40 kV and 11 μA for a 60 second count time, with a Ti-Al energy filter.

The compositional data from each well were then run through a hierarchical clustering analysis using the Spotfire software in order to cluster similar data based on their elemental signatures (Baumgardner and Rowe, 2017; Phillips, 1991; Rowe et al., 2017). The clustered data creates chemofacies, which are analogous to lithofacies in stratigraphy but are based on the chemical makeup of the samples (Elias and Alderton, 2020). This clustering analysis arranges %Si, %Al, %S, %Fe, %Mn, %Mg, %Ca, and %P in a hierarchical heat map (Table 1). A heat map is very similar to a cross table but contains colors instead of numbers. For this project, any element that is very low in concentration in a given sample is assigned a dark blue color, while

an element that is very rich in a sample receives a bright red color. Any element that has a mid-range value has a light grey color. As a result, there is a color gradient between the extremes of chemical content. Each of the heat maps contains a dendrogram on the left side. A dendrogram is a tree-structured graph, which helps the relationship and similarity between the chemical makeup of different samples to be understood. A line that runs through the dendrogram and can be dragged left or right in order to decide how many clusters are appropriate based on the patterns seen in the heat map (Baumgardner and Rowe, 2017) (Table 1).

Once clusters are determined, the elemental abundances are analyzed in order to understand the chemical makeup so that we can define each chemofacies (Table 3). The elemental abundance is determined as being $\frac{Average\ Element\ per\ Cluster}{Average\ Element\ per\ Study}$. When analyzing the elemental abundance per cluster in this way, any element with a number over one would be considered to have an overabundance, and any element with a number under one would be considered to have an underabundance. Each chemofacies can confidently named based on what elements are in an overabundance in each cluster. For example, if one cluster has a Ca abundance of 4.29 and every other element an abundance below 1.0, then that cluster can be labelled as a carbonate chemofacies.

Table 1. Heat map and clustering to create the chemofacies. The clusters are based on the similarity of their elemental signatures.

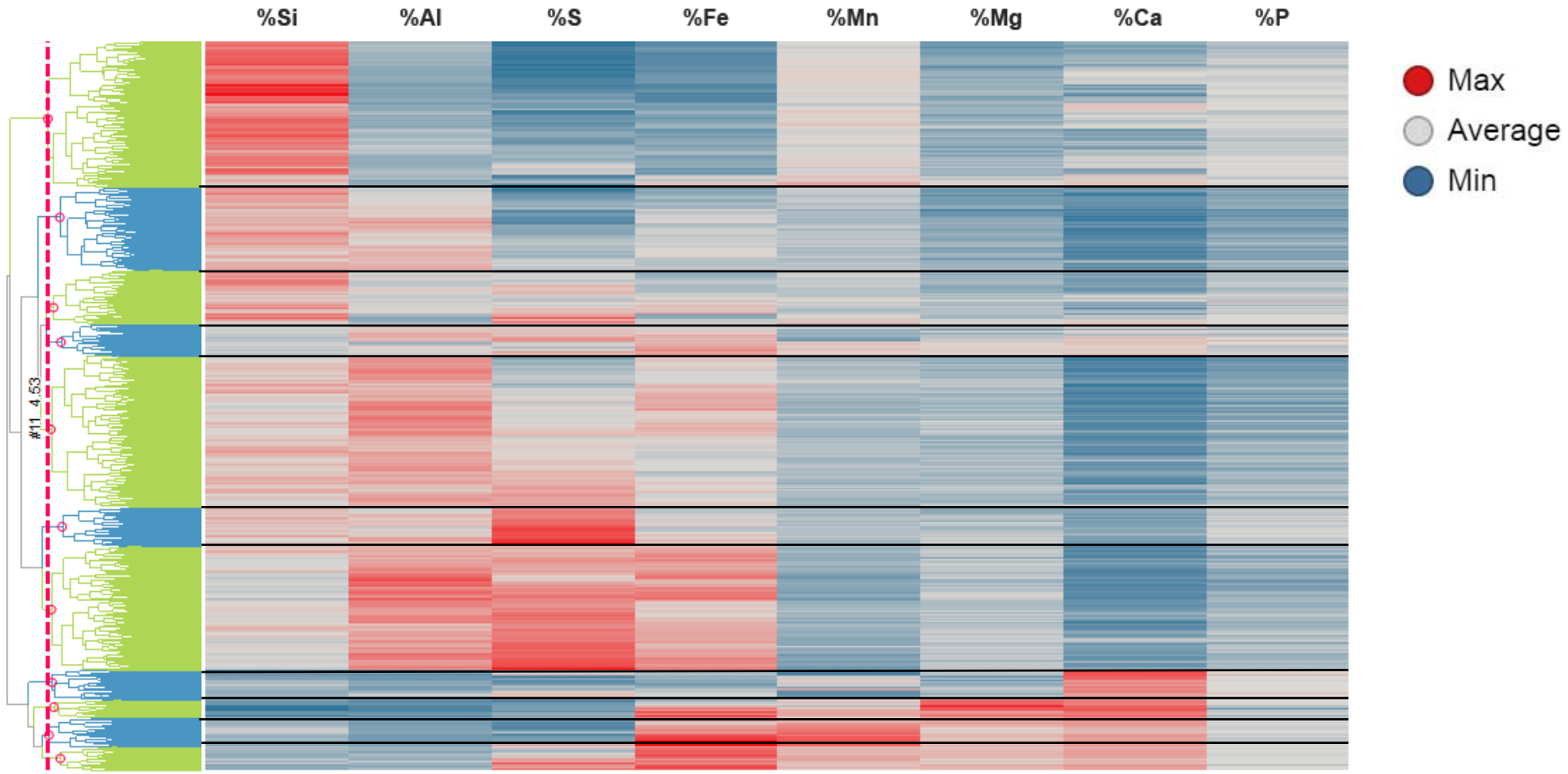

4.2. Correlation

After all the chemofacies are established in each well, a correlation of the chemofacies through all the wells was completed. This correlation was accomplished using Petrel. Petrel is a software developed by Schlumberger that is mostly used in the exploration and production part of the petroleum industry. It provides a platform for interpreting seismic data, performing well correlation, building reservoir models, creating volumes, and producing maps. In Petrel, the chemofacies data were uploaded as well logs where the chemofacies are plotted with depth. Once, that had been accomplished the geochemical data were correlated throughout all the wells.

Once all the data were uploaded the correlation began from the top to the bottom of the stratigraphy. Because the nine chemofacies alternated so often I grouped them into three groups, a siliciclastic group, a calcareous group, and a clay-rich group. This grouping allowed for a more generalized understanding of the lithofacies changes. A closer look at the changes between all of the chemofacies was done locally on each well.

4.3. Sequence Stratigraphy

Sea level variations, driven by waxing and waning of continental glaciation, are known to have occurred during the Late Pennsylvanian and Early Permian and to have affected the Midland Basin (Silver and Todd, 1969). Consequently, correlation between the chemofacies and sea level variation might be expected. Because of the large variations in sea level during the Early Permian, significant changes are expected from transgression to regression in the chemofacies. As sea level rises and transgression occurs, I predict a lithofacies pattern of sandstones, grading up to shales, and then carbonates in the basin center. This change in

lithofacies is due to the depositional environment changing as the sea level rose, with sands being sequestered on the shelf as the sea level rises. Once the sea level started to fall and regression occurred, the expected lithofacies pattern should be the opposite found during the transgression, with the lithofacies starting with carbonates, shales, and then sandstones at the end of the sequence. Falling sea level causes erosion and channel incision on the shelf and the transport of coarse clastics into the deep water.

Because there are few age constraints on the geochemical data, simple interpretations of the basin conditions were completed for each major geochemical change that occurred in the basin. After correlation was the study area was completed and the formation boundaries were determined, major shifts in the chemostratigraphy became apparent. These shifts were then compared and connected to the major changes in glacial volume and eustatic sea level of the Permian. This allowed for obvious periods of highstands, lowstands, and transgression (Fig. 5) (Fig. 9).

CHAPTER 5. RESULTS

5.1. Geochemistry

A total of 75,460 XRF data points were taken from the eleven wells evaluated during this study. The %Si, %Al, %S, %Fe, %Mn, %Mg, %Ca, and %P were taken from the 75,460 XRF measurements and were processed through a hierarchical clustering analysis in Spotfire in order to create statistical clusters. This created a heat map with a correlating dendrogram that was used to objectively decide how many clusters were found in this study. Eleven clusters were found in this study based on the similarities found within each % element in the heatmap. The elemental abundances of each cluster were analyzed in order to create the eleven chemofacies used in the interpretation. These eleven chemofacies include, Sandstone-Siltstone, Sulfur-Phosphorous Siltstone, Limestone, Pyritic-Phosphorous Marl, Dolomite, Iron-Manganese Dolomitic Limestone, Manganese-Iron Dolomitic Limestone, Silty Pyritic Mudstone, Oxic Mudstone, Pyritic Mudstone, and Phosphorus-Sulfur Mudstone (Table 3). The determination of how these chemofacies are defined is provided in the discussion.

For a more general understanding, the chemofacies were grouped into four groups (Table 2). The siliciclastic group contains the Sandstone-Siltstone and Sulfur-Phosphorous Siltstone chemofacies, the calcareous group contains the Limestone and Pyritic-Phosphorous Marl chemofacies, the dolomitic group contains the Dolomite, Iron-Manganese Dolomitic Limestone, and Manganese-Iron Dolomitic Limestone chemofacies, and the clay group contains the Silty Pyritic Mudstone, Oxic Mudstone, Pyritic Mudstone, and Phosphorus-Sulfur Mudstone chemofacies. The Wolfcamp Formation comprises 2.49% of the siliciclastic group, 1.78% of the carbonate group, 1.48% of the dolomitic group, and 94.25% of the clay group. The Dean Unit

contained 4.92% of the siliciclastic group, 5.36% of the carbonate group, 3.29% of the dolomitic group, and 86.43% of the clay group. The Spraberry Unit contained 16.07% of the siliciclastic group, 2.58% of the carbonate group, 6.46% of the dolomitic group, and 74.88% of the clay group (Table 4).

Table 2. This is a chart of all of the chemofacies broken down into their chemofacies groups. This is based on if the chemofacies is primarily, siliciclastic, calcareous, dolomitic, or clay rich.

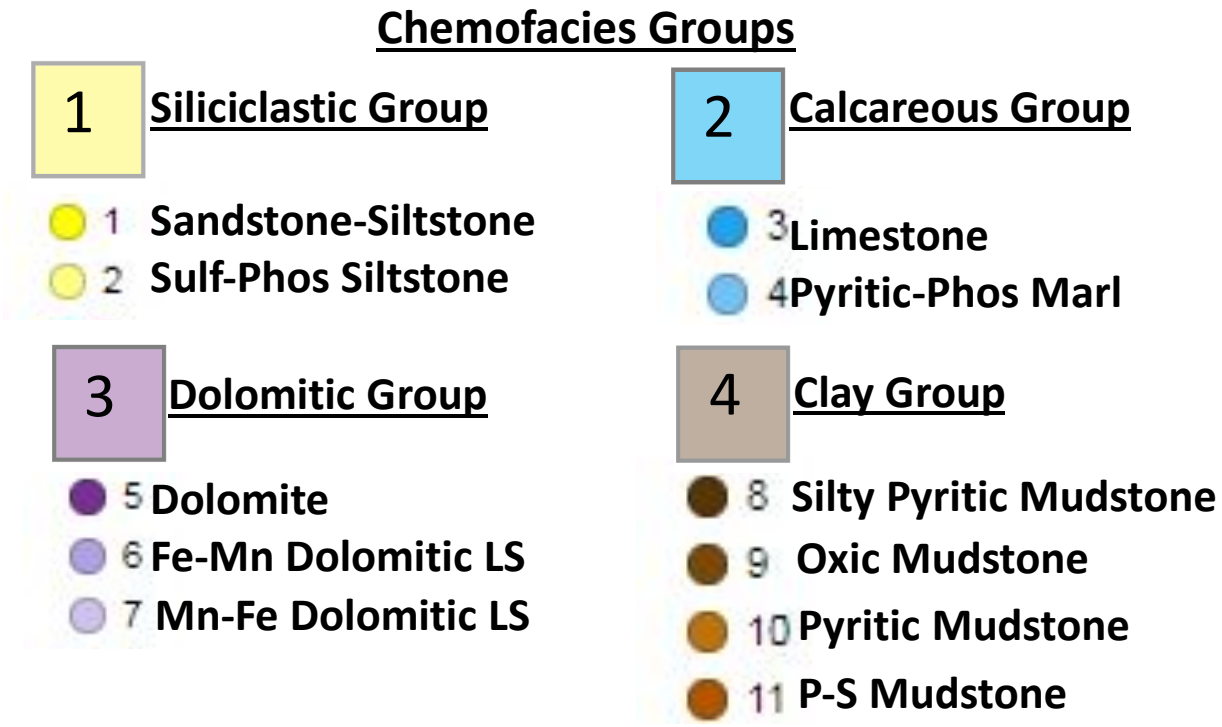

Table 3. Elemental abundance of each chemofacies. Calculated by $\frac{Average\ Element\ per\ Cluster}{Average\ Element\ per\ Study}$.

1.Sandstone-Siltstone		2. Sulf-Phos Silstone		3. Limestone		4. Pyritic-Phos Marl		5. Dolomite		6. Fe-Mn Dolomitic LS	
%Si	1.17	%S	1.13	%Ca	4.29	%Ca	1.44	%Mg	6.47	%Ca	2.78
%Mn	1.08	%Si	1.09	%Mn	0.88	%Fe	1.23	%Ca	4.59	%Mg	2.49
%Ca	0.86	%Mn	0.98	%S	0.80	%S	1.16	%Mn	1.38	%Fe	1.75
%Al	0.67	%K	0.90	%Mg	0.75	%Mg	1.08	%Fe	1.34	%Mn	1.49
%Mg	0.65	%Al	0.89	%Fe	0.70	%Al	1.04	%S	0.49	%S	1.27
%K	0.64	%Fe	0.85	%Si	0.66	%K	1.00	%Si	0.42	%Si	0.73
%Fe	0.48	%Mg	0.74	%Al	0.57	%Mn	0.99	%Al	0.38	%Al	0.68
%S	0.46	%Ca	0.70	%K	0.47	%Si	0.90	%K	0.36	%K	0.59

7. Mn-Fe Dolomitic LS		8. Silty-Pyritic Mudstone		9. Oxic Mudstone		10. Pyritic Mudstone		11. P-S Mudstone	
%Ca	2.98	%K	1.31	%K	1.12	%S	1.63	%S	1.93
%Mg	2.59	%Al	1.28	%Al	1.10	%K	1.40	%K	1.11
%Mn	2.21	%Fe	1.08	%Si	1.08	%Fe	1.37	%Al	1.09
%Fe	1.69	%S	1.05	%Mn	0.89	%Al	1.35	%Si	1.04
%Si	0.75	%Si	1.03	%Fe	0.82	%Si	0.97	%Fe	0.97
%S	0.53	%Mn	0.86	%S	0.61	%Mg	0.83	%Mn	0.88
%Al	0.52	%Mg	0.73	%Mg	0.54	%Mn	0.79	%Mg	0.78
%K	0.44	%Ca	0.38	%Ca	0.33	%Ca	0.43	%Ca	0.53

5.2. Correlation

Correlation of the chemofacies in all eleven wells was completed across the study area and two cross sections of the study area were interpreted using the correlated data. The first cross section is oriented East-West along wells four, five, and six. The second cross section is oriented South-North cutting through the middle of the study area. In the Wolfcamp and Dean units, mud is prominent with sandstones, carbonates, and dolomites being deposited in the Northwest region of the study area and pinching out about 6–9 km south of the northernmost point of the study area and 9–11 km east of the westernmost point of the study area. The East-West oriented cross-section also contains two sand packages around 2.5 km below sea level that begin and pinch out towards the southeast within the cross section (Fig. 8). These same two sand packages are seen in the South-North oriented cross section but must originate beyond the northern boundary of the study area. Within the Spraberry Unit, the thicker lithologic units seem to correlate throughout the whole study area while the thinner lithologic units tend begin and pinch out within the study area (Fig. 8). There are many more of these thinner lithofacies packages found in the South-North oriented cross section, specifically south of where the two cross sections cross one another.

5.3. Sequence Stratigraphy

The Spraberry Unit experienced far more frequent sea level fluctuations than the earlier units, the Wolfcamp and Dean (Fig. 8). During Wolfcamp times different chemofacies were deposited but the sequences are dominated by chemofacies in the clay group (Table 4). During sedimentation of the Dean, fluctuations did occur but each sea level change lasted a longer time than its predecessor and was not continuous over the whole study area. The Upper Wolfcamp

was deposited during a period of glacial maximum, and therefore relatively low sea level. This period was followed by a trend towards sea level rise, which is why the Upper Wolfcamp represents a lowstand unit (Shanmugam, 2018). During the Dean the first major change towards sea level rise occurred, which is exhibited by the first transgression into the carbonate unit that is seen in both cross sections (Fig. 9). After this initial episode of transgression, there were alternating episodes of regression and transgression that are evidenced by the two sandstone units that have been mapped through the northwest portion of the study area. Although the Dean has cycles of transgression and regression, it experienced a general shift to increased carbonate contents. Therefore, the Dean is interpreted to represent a general trend of transgression.

Following the Dean, the Lower Spraberry started with a rapidly rotating episode of transgression and regression, as indicated by the five carbonate units with clay units between them found between 2.4 and 2.5 km below sea level on the East-West oriented cross section (Fig. 8). This section again shows a transgressive trend. Next, the fluctuations in sea level began to become more frequent and occurred over shorter intervals of time. The rate of sea level rise began to decrease at this point and there were more frequent periods of regression, which is indicative of a highstand systems tract (Fig. 9)(Bertram, 2012).

CHAPTER 6. DISCUSSION

6.1. Geochemistry

Each chemofacies was decided on and named based on the percent element found in each one. Referring back to the geochemical section in the methods, any abundance over 1 is considered high in this study because the elemental abundance is calculated by $\frac{\text{Average Element per Cluster}}{\text{Average Element per Study}}$ The siliciclastic group contains the sandstone-siltstone chemofacies and the Sulfur-Phosphorus chemofacies. The sandstone-siltstone chemofacies is high in silica and with an above average presence of Manganese. I believe this chemofacies was deposited in a deep-water environment, if a thick bed of sandstone-siltstone chemofacies was deposited it was supplied from submarine-fan channels and lobes but I intepret thinner beds to represent sedimentation on channel levees and turbidite sheets (Hamlin and Baumgardner, 2012). The sulfur-phosphorus siltstone is high in silica, sulfur, and with an average Phosphorus content of 1.27%. Because phosphorus is essential to life and is linked to organic matter, I interpret the depositional environment of this chemofacies to have been shallower than the deep-water environment that the sandstone-siltstone chemofacies was deposited in but still brought into the basin by submarine fan channels, lobes, channel levees, turbidite sheets, or mass transport deposits (Craigie, 2018).

Two chemofacies are in the calcareous group, the limestone chemofacies and pyritic-phosphorus marl chemofacies. The limestone chemofacies is almost pure calcium. Calcium is the only element with an abundance over 1. Not only is it over 1, it is significantly over one at 4.29. Limestone was decided for the name because of the high calcium abundance. The study area is known to have been a deep-water environment that was conducive to carbonate deposition (Fig. 6). The second chemofacies in the calcareous group, the pyritic-phosphorus marl, is a marl

because marls are a rock that contains both carbonate and clay. The clay content of a marl is anywhere between 20% and 80% of the rock and calcite is somewhere between 20% and 80% of the rocks composition also (Haldar, 2020). This chemofacies has a high calcium abundance of 1.44 and also aluminum and potassium are over 1 which indicates that clays are also largely present in this chemofacies. It was also important to note that pyrite is present in this chemofacies. Pyrite's chemical composition is FeS_2, the iron abundance in the chemofacies is 1.23 on average and the sulfur is 1.16. The chemofacies is also high in phosphorus with an average abundance of 2.13. Marls are usually formed during quick oscillating cycles between a wet and dryer environment, commonly changes on the scale of months (Hillel and Hatfield, 2005).

The dolomitic group consists of three chemofacies, Dolomite, Iron-Manganese Dolomitic Limestone, and Manganese-Iron Dolomitic Limestone. All of these chemofacies are in the dolomite group instead of the calcareous group because they all have a high Magnesium contents. The dolomitization that occurred in this study area is considered to have occurred fairly soon after the deposition of the carbonate and was caused by hypersaline brines that developed in supratidal settings (Adams and Rhodes, 1960; Craigie, 2018). Because all of the chemofacies in the dolomitic group were deposited as carbonate, they have a very similar depositional environment as the limestone chemofacies but then became dolomite when the environment transitioned to an evaporite lagoon. I do not believe that these chemofacies could have been deposited in basin but brought into the basin through mass transport deposits. During this time, the basin never became shallow enough for a supratidal setting to develop. The dolomite chemofacies is extremely rich in magnesium and calcite. It also contains a high content of manganese and iron, but in this chemofacies the percentage of each is almost equal. The next

chemofacies, iron-manganese dolomitic limestone contains high concentrations of both calcium and magnesium. The iron content found in this chemofacies is higher than the manganese. Sulfur is also rich in this chemofacies, but not close enough to the amount of iron found in the chemofacies for pyrite to be present. The manganese-iron dolomitic limestone has similar calcium and magnesium contents as the iron-manganese dolomitic limestone but far more manganese than iron. The sulfur abundance of this chemofacies is below 1, so that no pyrite is present.

The clay group consists of four chemofacies, the silty pyritic mudstone chemofacies, the oxic mudstone chemofacies, the pyritic mudstone chemofacies, and the phosphorus-sulfur mudstone. The silty pyritic mudstone chemofacies has a high amount of potassium and aluminum with a silica content higher than 1%. The presence of silica reflects the fact that the chemofacies is silty. There are also very similar iron and sulfur contents in the chemofacies, suggesting that pyrite is present in the chemofacies. Pyrite can be observed in cuttings but it is important to look at the chemical make up of the cuttings to confirm it is pyrite. Unfortunately, a lot of times trash or remints from the drilling equipment gets mixed in with the cuttings. The presence of pyrite is normally indicative of an anoxic, reducing environment. A study looking at black shale deposition and early diagenetic dolomite cementation during an oceanic anoxic event suggests that anoxic shales are probably deposited during sea level lowstands (Petrash et al., 2016). The oxic mudstone chemofacies has a similar composition to the silty-pyritic mudstone, with high potassium, aluminum and silica, expect it is lacking iron and sulfur, so that there is no presence of pyrite in this chemofacies. The presence of pyrite is usually a good indicator of an anoxic environment, therefore the lack of pyrite suggests an oxic environment (Craigie, 2018). An oxic depositional environment for mudstones that contain silica outside of the basin would be

a lagoonal setting (Petrash et al., 2016). These then would be deposited into the basin by mass transport deposits.

The pyritic mudstone chemofacies has high potassium and aluminum abundances, indicative of any mudstone but the silica is below 1. This chemofacies also has a high amount of sulfur and iron present, reflect the presence of pyrite in the chemofacies. Just like in the silty-pyritic mudstone chemofacies, the pyrite present in the pyritic mudstone suggests an anoxic depositional environment (Craigie, 2018). The last chemofacies, the phosphorus-sulfur mudstone which is high in potassium, aluminum, and silica. Because silica is present, it is more of a silty mudstone. There is also a high amount of sulfur present in this chemofacies but iron is low. Therefore no pyrite is present in this mudstone. Just as for the oxic mudstone chemofacies, this mudstone was also probably deposited in an oxic environment. It was also important to note that the phosphorus abundance is about 1. Phosphorous is essential to life and is linked to organic matter, this is just another justification as to why the phosphorus-sulfur mudstone was deposited in an oxic environment. (Craigie, 2018).

6.2. Correlation

Correlation throughout the study shows the drastic changes in lithologies found in each formation. 94.25% of the chemofacies found in the Wolfcamp are in the clay chemofacies group, 3.26% are in the carbonate and dolomite group, and the other 2.49% are from the siliciclastic group (Table 4). Because there is such a high percentage of clays in this formation, this suggests that the sea level was at a high point and the study area was positioned in a shallow sea. The small amount of carbonates and sands found in this formation are not continuous and came from erosion from the carbonate shelves.

The Dean Formation consists of a larger amount of both sandstone and carbonate. The clay chemofacies group percentage dropped from about 94% to 86.43% in the Dean Formation, and the siliciclastic chemofacies group increased to 4.92% and the carbonate and dolomitic chemofacies group increased to 8.65% (Table 4). There is a decrease in glacial volume during Dean Formation sedimentation and therefore an increase in eustatic sea level (Fig. 9). At the same time as sea level was rising, subsidence was occurring in the basin and the South American Margin was moving towards the northwest, slowly decreasing accommodation space (Fig. 3). The increase in eustatic sea level along with subsidence created a deep enough environment for increased carbonate production. The clastic sedimentation, including the siliciclastic chemofacies were deposited by feeder channels and submarine canyons (Frenzel et al., 1988; Handford, 1981).

The Spraberry Formation follows a similar trend as the Dean Formation. The clay chemofacies group again decreased to only 74.88% of the total chemofacies found in the Spraberry (Table 4). The siliciclastic chemofacies increased to 16.07% and the carbonate and dolomite chemofacies increased to 9.04% of the total chemofacies in the Spraberry. The siliciclastic chemofacies and carbonate chemofacies are mostly correlated throughout the study area. Each facies layer is much thinner than in the previous formations. This is due to the decreasing accommodation space along with the increasing eustatic sea level. These two factors caused frequent variation in local sea level.

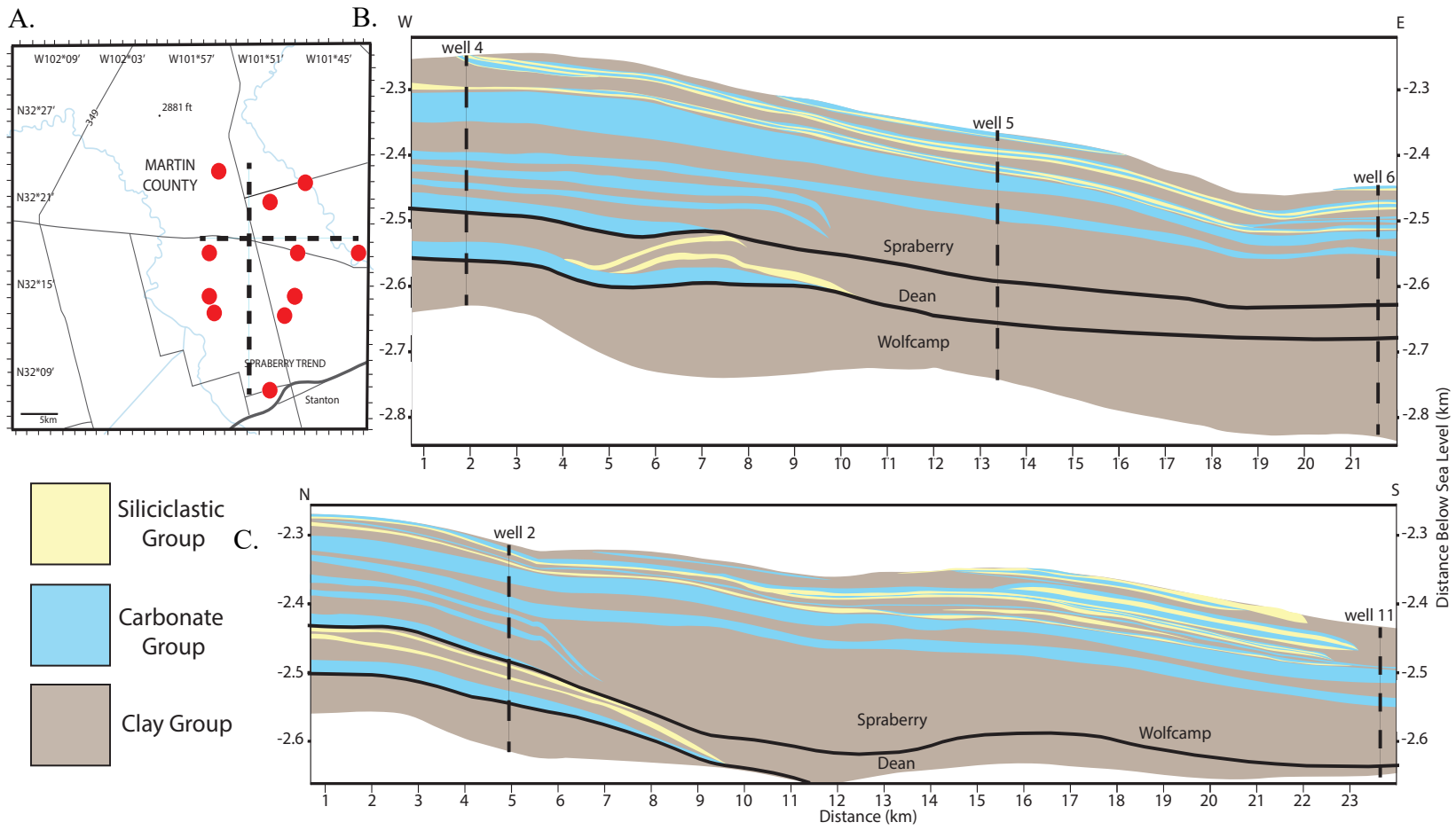

Figure 8. The chemostratigraphic correlation shown in two different cross sections. **(A)** Map of Martin County with all eleven wells in the study marked by red dots. The two cross sections are represented by the dashed lines **(B)** cross section runs east west through the study area. **(C)** cross section runs north south through the study area.

Table 4. The overall abundance of each chemofacies group in each formation. The Wolfcamp has 94.25% clay chemofacies, 3.26% calcareous chemofacies, and 2.49% siliciclastic chemofacies. The Dean has 86.43% clay chemofacies, 8.65% calcareous chemofacies, and 4.92% siliciclastic chemofacies. The Spraberry 74.88% clay chemofacies, 9.04% calcareous chemofacies, and 16.07% siliciclastic chemofacies.

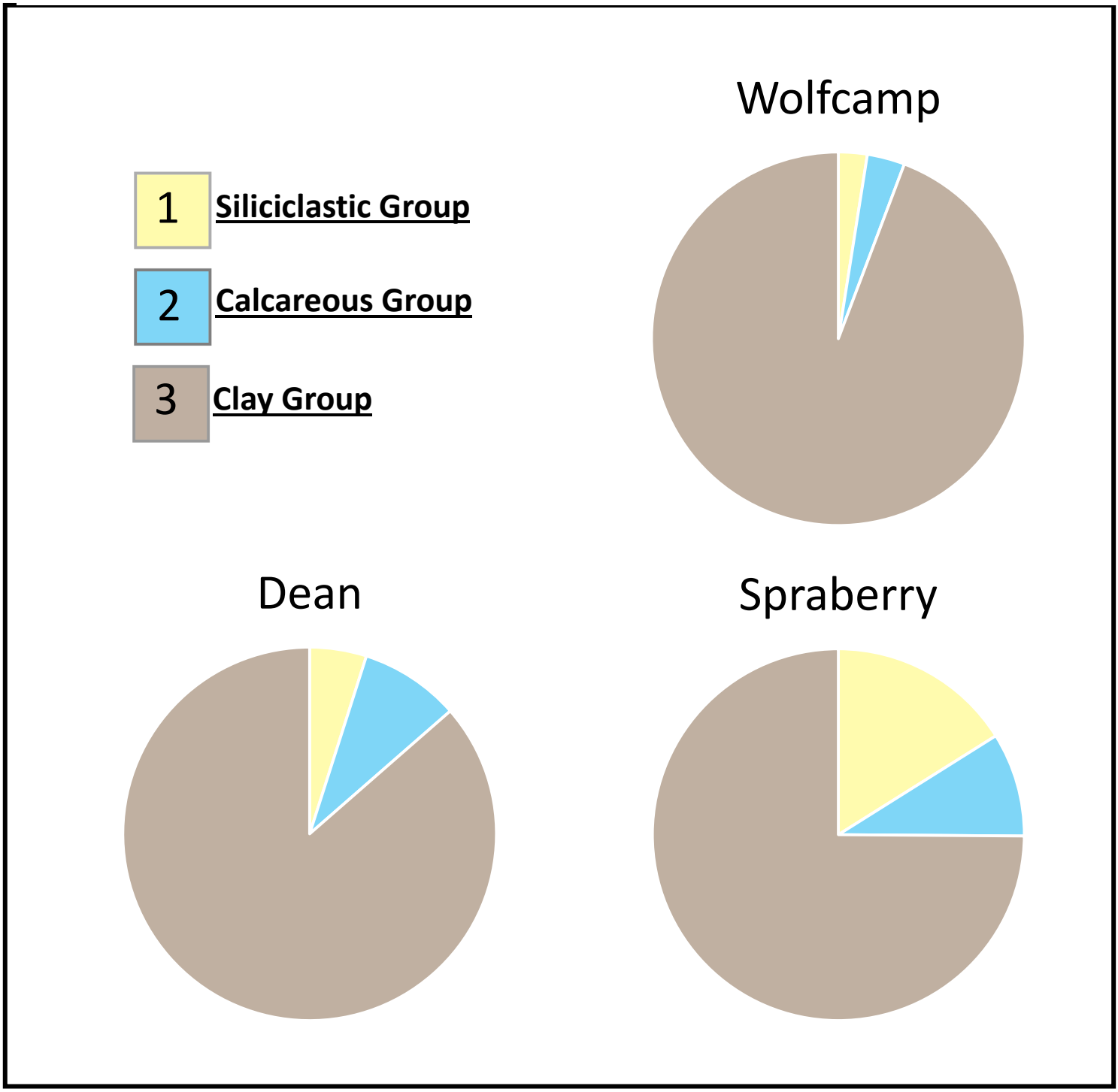

6.3. Sequence Stratigraphy

It is difficult to determine sequence stratigraphy through geochemical core and cuttings-based studies alone. Time-event stratal connections make it difficult to provide specific sequence stratigraphy because geochemical signatures represent changes in the sedimentation at the bottom of the marine basin. When this deposition occurred at a distance from the sediment source, there can be a sizable lag in time between environmental changes and deposition of the sediment (Cortez, 2012). The lag times can also substantially vary depending on the type of deposition. For example, although most times falling sea level reduces accommodation space, there are instances where increased accommodation and erosional capacity of a basin can occur at the same time as sea level fall. Also, trace metal accumulation from the same sea level fall event could occur much later after the fall commences. This makes the correlation of depositional events with time quite ambiguous. Because of this limitation, traditional sequence stratigraphy systems tracts are not defined, but simple interpretations of the basin conditions are discussed for each major geochemical change that occurred in the basin.

The chemostratigraphy of this study that was correlated throughout the study area specifies where shifts in depositional environment have occurred. These shifts combined with basin dynamics and paleoclimate provide reliable possibilities for sequence stratigraphy boundaries for this study. The upper Wolfcamp was influenced to a greater degree by subsidence than the Leonardian (Mazzullo et al., 1989). Based on past studies and the degree of basin restriction, the system is interpreted to be eustatic driven (Crowell, 1978; Mazzullo et al., 1989; Veevers and Powell, 1987). The primary factor affecting the sea level is the Late Paleozoic glaciation.

The Late Paleozoic Ice Age influenced the global sea levels from the Mississippian through the Permian (Fig. 5) (Blakey and Fielding, 2008; Fielding et al., 2008). During the Late Pennsylvanian global temperatures dropped, which caused development of greater volumes of glaciers from the poles down to the lower latitudes (Fielding et al., 2008). This increase in glacial volume caused a rapid sea level drop, which created a sediment that has similar characteristics as those formed during a lowstand (Fig. 9). Because the Midland Basin is located near the equator, the basin was subject to high rates of erosion (Blakey and Fielding, 2008; Fielding et al., 2008; Flamm, 2008; Mazzullo et al., 1989). Glacial erosion rates are higher in lower latitudes because of the climate control on basal temperature and increased meltwater. The increase of meltwater promotes glacial sliding, erosion, and sediment transfer (Koppes et al., 2015). Because of the rapid erosion, low sea levels contributed to two prominent situations. The first is an increase in an incising erosional front, which caused greater resedimentation of the shelf carbonates into the basin. The second is increased basin restriction which hindered circulation within the basin (Cortez, 2012).

As the Pennsylvanian progressed towards the Leonardian, there was an increase in the presence of the siliciclastic chemofacies groups. At first, I believed this was due to an increased presence of debris flows and turbidites. But this cannot be correct because turbidity currents are most commonly associated with sea level fall but the Leonardian Formation was experiencing sea level rise and basin subsidence (Bhatnagar et al., 2018; Shanmugam and Moiola, 1982). The assumption of eustatic sea level rise is also seen in the Late Paleozoic Ice Age estimates that show a drastic decrease in ice volume, followed by a steady decline (Fig. 5). Instead of the increasing siliciclastic sediment input being due to turbidity currents, it must be due to an increase in mass transport deposits (Bhatnagar et al., 2018). Mass transport deposits are known

to occur in deep water settings (Moscardelli and Wood, 2016; Posamentier et al., 2011). The increased erosion of the carbonate factories along the continental shelf deposited sediment that is dominated oxygenated calcium and iron. This event is labelled Transgression 1 in Figure 9, and also records a shift around the Dean Formation in sediment character as the shore face approached a terrigenous sediment source of differing character. There is also a general change in the chemical character away from Calcium to Potassium. This shift is indicative of the coastline moving inland past the shelf carbonate factories, advancing past the former beach front.

Moving into the Early Permian, there is a shift from an anoxic to euxinic bottom water. This transition, marked by Transgression 2, correlates with increased ice reduction. This transition from anoxic to euxinic occurs because of the restricted access of the basin to the open ocean seen by the tectonic shift that occurs at the early Permian (Fig. 3). Although this transition occurred in a general trend of transgression, there was still a major shift in basin dynamics at that time. The modest amount of tectonic activity that occurred during the Spraberry could have caused a diversion of sediment that resulted in less accommodation space and erosion outside of the basin. The decrease in detrital sediment favored an increase in the production of carbonate. There was still nutrient input that occurred elsewhere, increased the biologic activity throughout the basin. This increased the amount of carbonate seen throughout this section of the study.

The uppermost portion of the area contains the only highstand condition of the studied intervals (Fig. 9). During this highstand there was a high degree of cyclicity that is seen both in the XRF measurements, lithologies and the glacial frequency. This trend is due to a long-term trend towards sea level rise. The global climate continued to become more arid, with the study area experienced increased aridity due to Gondwana and Laurasia coming together and the study area becoming landlocked. The alternating sea level would go back and forth from covering the

carbonate shelves and the previously eroded terrigenous terrain. This allows for the coarse grained carbonate debris from the shelves and the silica from the shorefronts to be deposited into the basin.

6.4. Future Work

Because the correlation between my wells involves kilometer-scale distances between the wells, there is a lot of area that is not accurately correlated. In order to have full certainty on the correlation between the wells, I would like to incorporate seismic data into any future work done on this study. This would allow for a more accurate correlation throughout the whole study area and to show more minute changes and variations within each chemostratigraphic layer.

In addition, both the total organic carbon and stable isotopes of organic carbon would be a welcome source of data for this project. This will not only create a better understanding about the potential hydrocarbons in the area, but also give a lot of background information on the depositional environment. Incorporating total organic carbon into the study would help support theories about the paleoclimate, paleoenvironment, and depositional processes (Dembicki, 2016; Slatt, 2013). The stable isotopes of organic carbon has been historically used to determine the provenance of organic matter in mudrocks and the paleo productivity and climatology of the mudrocks depositional environment (Meyers, 1994, 1997; Meyers et al., 2009). This will help to further recognize the oxygen fluctuation that took place.

Lastly, in future studies I would look into more of the redox sensitive elements. These elements include trace metals vanadium, chromium, titanium, molybdenum, nickel, and zinc. These are good indicators of oxygen concentrations in the depositional waters. For example

molybdenum is a good indicator of a suboxic-euxinic depositional environment (McManus et al., 2006).

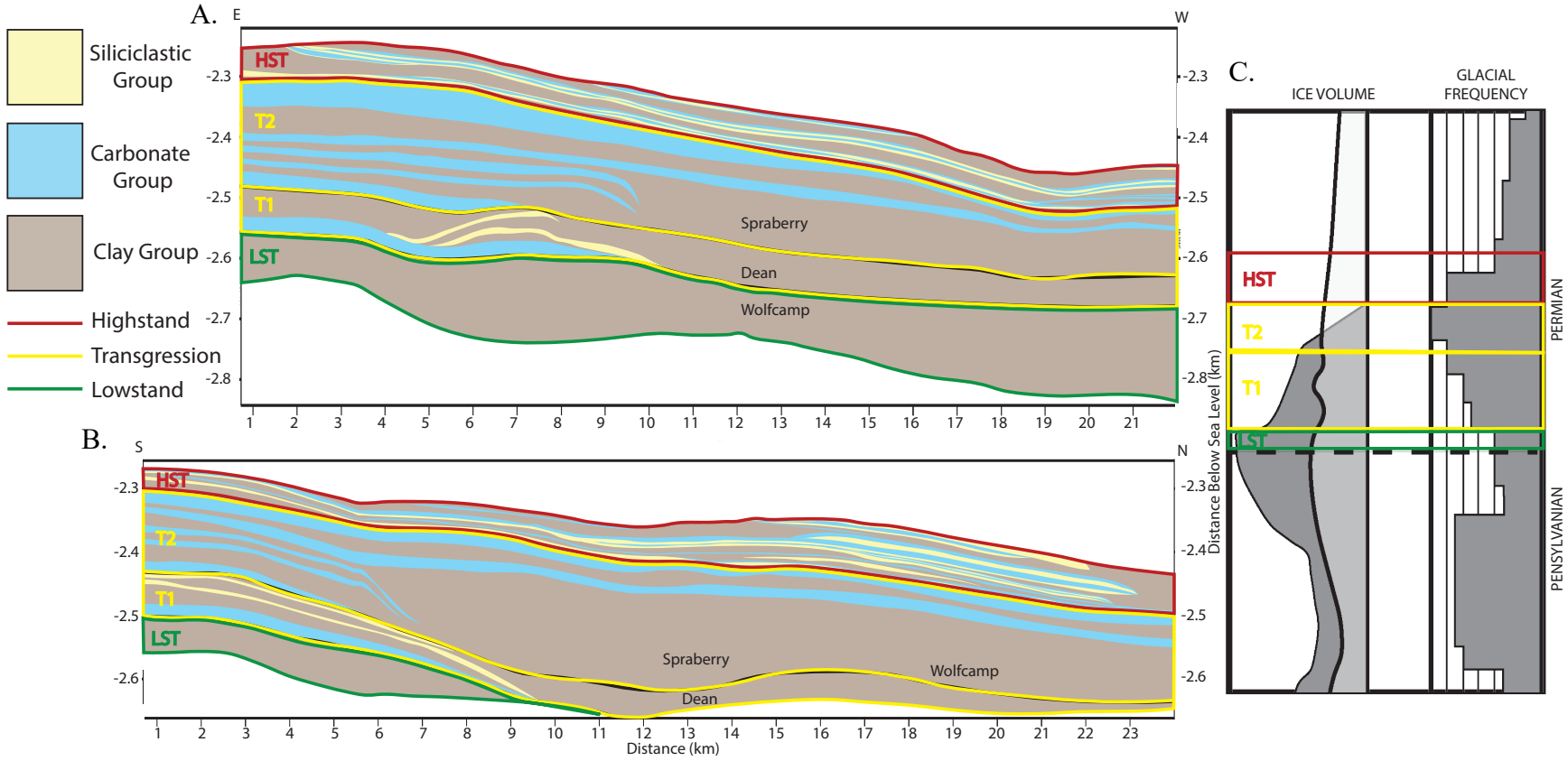

Figure 9. The chemostratigraphic correlation shown in two different cross sections. Each cross section is broken into their sequence stratigraphic systems. LST stands for a lowstand systems tract, T1 stands for the first transgression, T2 stands for the second transgression, and HST stands for the highstand systems tract. **(A)** cross section runs east west through the study area. **(B)** cross section runs north south through the study area. **(C)** Stratigraphic range chart showing interpretations of the extent of glaciation through the Carboniferous and Permian System (Crowell, 1999; Fielding et al., 2008; Frakes et al., 1992; Veevers and Powell, 1987). The sequence stratigraphic systems are represented here also.

CHAPTER 7. CONCLUSION

7.1. Hypothesis Analysis

-Question 1: Do changes in lithology correlate with known changes in sea level?

-*Hypothesis 1:* The Late Pennsylvanian and Early Permian were icehouse periods with smaller fluctuations in sea level due to the melting and rebuilding of ice sheets. The changes in lithology found through the Upper Pennsylvanian and Lower Permian should represent the large scale changes in sea level that occurred over this time.

-This hypothesis was proved correct by the increased carbonate content that was deposited as glacial volume decreased and eustatic sea level increased

-Question 2: Is there are a major shift in lithology when the climate changes from glacial to interglacial?

-*Hypothesis 2:* It is known that there was an icehouse period during the Late Pennsylvanian and Early Permian with many smaller episodes of heating and cooling (Baumgardner et al., 2016). One of the major warming events that occurred during this time is at the Pennsylvanian-Permian boundary. Following this event, the climate began to trend towards aridity. I expect to see a large shift towards shales and carbonates after the Pennsylvanian-Permian boundary driven by reduced erosion onshore.

-This hypothesis is partially correct, the amount of carbonate increased but the amount of clay chemofacies decreased. The amount of silica dominated chemofacies also increased which is due to an increase of mass transport deposits into the basin.

-Question 3: Can small changes in lithology be correlated between wells?

-*Hypothesis 3:* The Wolfcamp and Spraberry units are highly heterolithic. Some of these changes in lithology occur at an inch scale. It is unknown if these small changes in lithology are localized or seen throughout the region.

-Many of the small scale changes were for such a small thickness that it became very difficult to try to correlate every little change in chemofacies throughout all eleven wells. Many of these small scale changes were localized and not seen in every well.

-Question 4: Can smaller oscillations of transgression and regression be predicted from changes in lithology in the deep basin?

-*Hypothesis 4:* Deposition during the Pennsylvanian and Permian, the area experienced fluctuations in sea level driven by the melting and rebuilding of glaciers. This caused repeated periods of regression and transgression. Based on the patterns found in the lithology of the Wolfcamp and Spraberry, these intervals of transgression and regression should be identifiable.

-The large scale changes in transgression and regression were identifiable. Because age constraints are difficult with geochemical data and it was difficult to correlate small scale changes in lithology and it was difficult to correlate small scale changes in lithology, it became difficult to identify small scale changes in transgression and regression

7.2. Concluding Thoughts

Through an integration of geochemical data, basin dynamics, and sequence stratigraphy this study provides an insight into the sea level fluctuations and paleoclimate of the Late Pennsylvanian and Early Permian in the Midland Basin. This work follows the reconstructed sea level trend from a high glacial frequency to a lower glacial frequency and a higher eustatic sea level (Fig. 5) (Fielding et al., 2008). The correlated geochemical data give a highly detailed

analysis of the clastic material deposited, which in turn provides greater insight into the impacts of sea level fluctuations on the evolution of the basin margin.

The XRF data from the Wolfcamp, Dean and Spraberry formations contain elemental compositions that are indicative of a dominantly detrital signature. All three formations are dominated by clay-rich units, but as the global ice volume began to decrease and the eustatic sea level increased the carbonates units began to increase. Fine scale elemental changes are related to the depositional processes that transported the sediments into the basin. The composition of each chemofacies is tied to the origin of the dominant grain type for each chemofacies unit. Areas with high silica and aluminum are deposited by silty/sandy turbidites and mud plumes on the basin floor and the basin floor fans. The carbonate chemofacies groups were deposited by bioclastic turbidities or carbonate debris flows that were coming from the carbonate platforms surrounding the basin.

The Late Paleozoic Ice Age influenced the global seas levels from the Mississippian through the Permian. During the Late Pennsylvanian, glacial volumes increased and began to cover the lower latitudes. The large volumes of continental glaciers created a global sea level drop, which caused a lowstand during the Late Pennsylvanian. Lowstand systems tracts are generally associated with siliciclastic sediments, but in this study the Wolfcamp consists of mostly clay chemofacies (Ainsworth and Pattison, 1994). This could be because the study area is located between lobes of siliciclastic sediment. As the glacial frequency began to decline during deposition of the Dean Formation, sea level began to rise. Increased amounts of turbidities and debris flows occurred concurrently with subsidence of the basin. The Dean Formation represents the first transgressive event of this study. The lower Spraberry Formation records a large decrease in ice volume and also a decrease in accommodation space. This decrease in

accommodation space decreased the availability for detrital input from erosion that occurred outside the basin and increased the production of carbonate. The section transgressive event of this study occurred during the lower Spraberry. The uppermost portion of this studied section experienced a highstand period, during which there is a high degree of cyclicity in chemofacies. This cyclicity is correlated to the trend towards sea level rise and the basin becoming more landlocked.

APPENDIX A. LIST OF WELL

Study Number	API	Well Name	Company	Latitude	Longitude
1	42-317-3401800	Caffey 1	Odessa Exploration Inc.	32.410063	-101.90037
2	42-317-3058500	Wurtz No. 1	Adobe Oil Company	32.34104	-101.83068
3	42-317-3218300	J.E. Peugh #1	R.K. Petroleum	32.366605	-101.7932
4	42-317-3425300	Epley 31 #2	Concho Resources	32.298575	-101.92598
5	42-317-3395400	Lost Dutchman #1	Collins & Ware, Inc.	32.292948	-101.80092
6	42-317-3419700	Lindsay #2	Devon Energy Production Co, L.P.	32.283922	-101.70752
7	42-317-3399700	Tunnell No. 2	Odessa Exploration Inc.	32.25159	-101.91454
8	42-317-3122000	D.E. Richards	Sun Oil	32.214747	-101.81427
9	42-317-3453000	Sale Ranch M #3	Pioneer Natural Resources	32.216962	-101.90398
10	42-317-3402800	Grisham-Greeman #44	John L. Cox	32.196984	-101.82674
11	42-317-3319500	Mc Clane # 1-A	FEF Oil Corp	32.130065	-101.8232

APPENDIX B. WELL LOGS

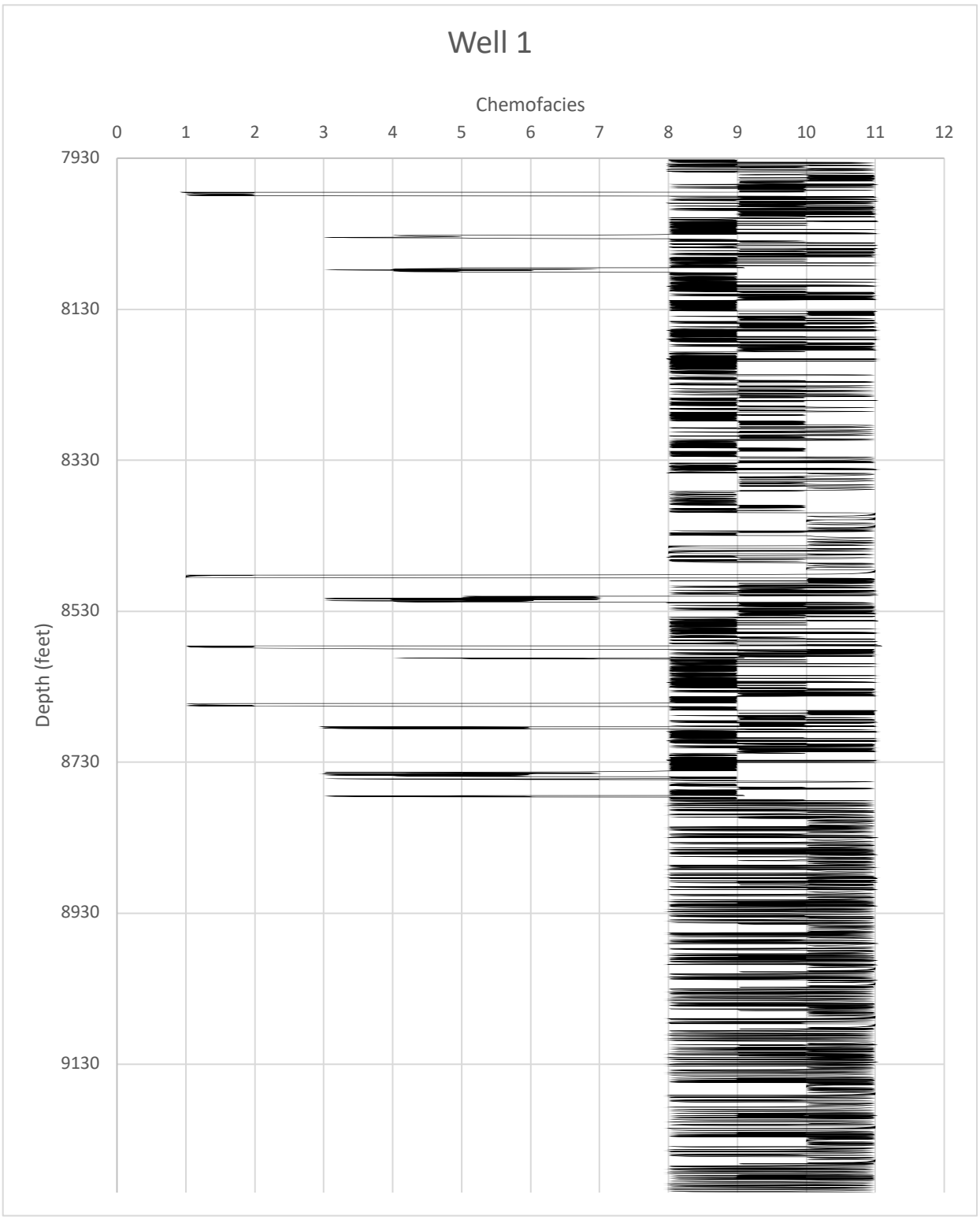

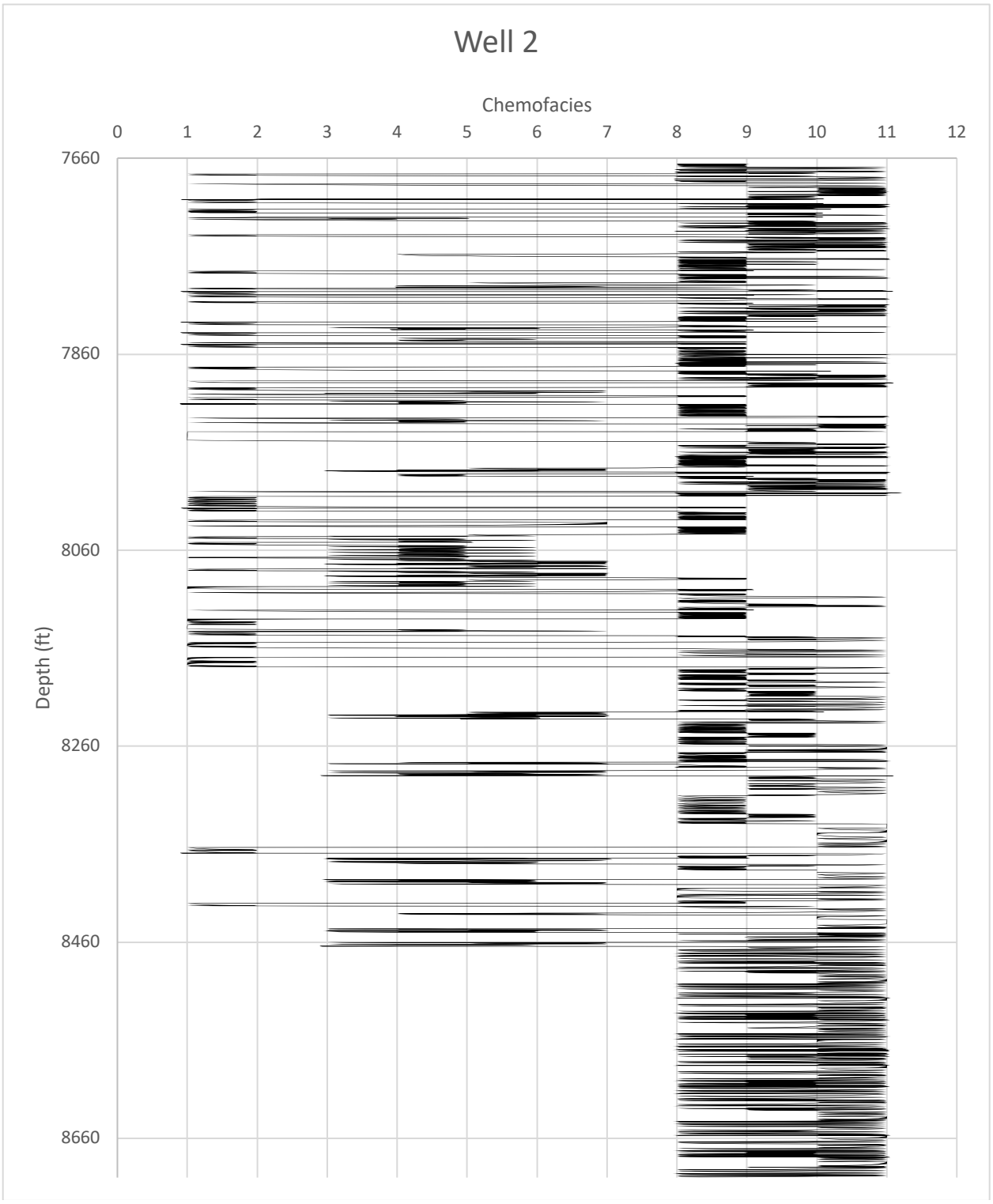
Well 2
Chemofacies
0
1
2
3
4
5
6
7
8
9
10
11
12
Depth (ft)
7660
7860
8060
8260
8460
8660

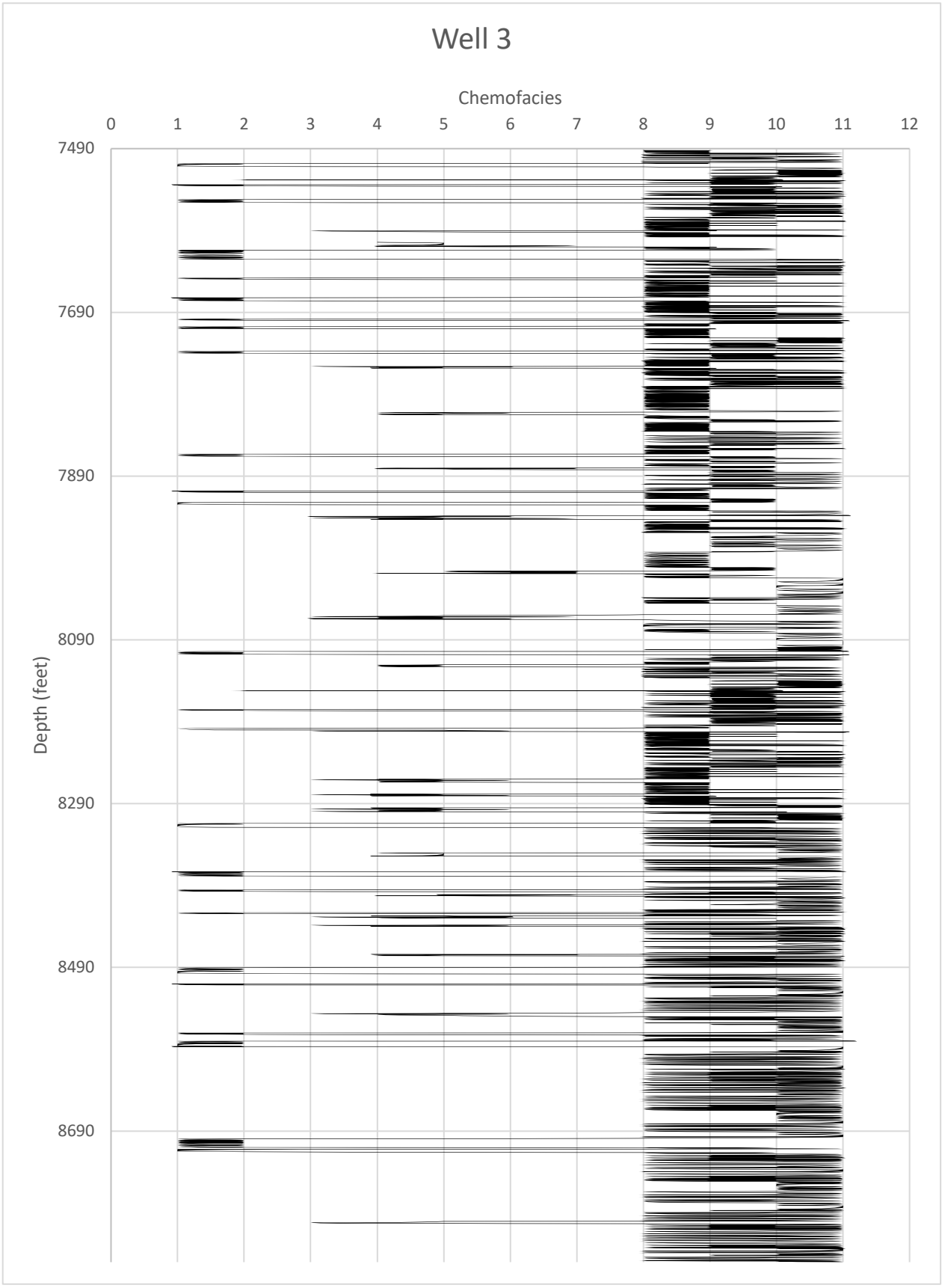
Well 3
Chemofacies
0
1
2
3
4
5
6
7
8
9
10
11
12
Depth (feet)
7490
7690
7890
8090
8290
8490
8690

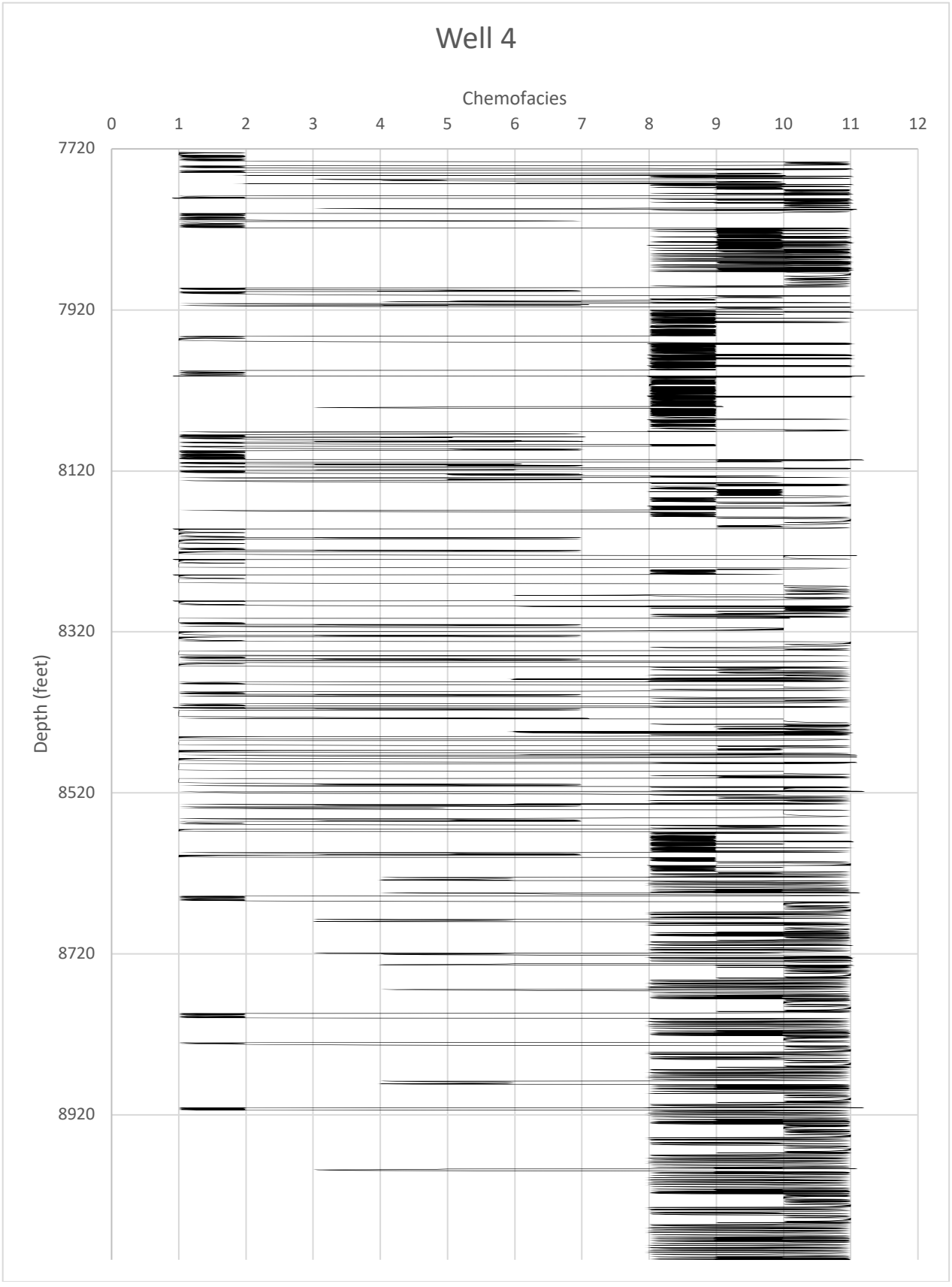
Well 4
Chemofacies
0
1
2
3
4
5
6
7
8
9
10
11
12
Depth (feet)
7720
7920
8120
8320
8520
8720
8920

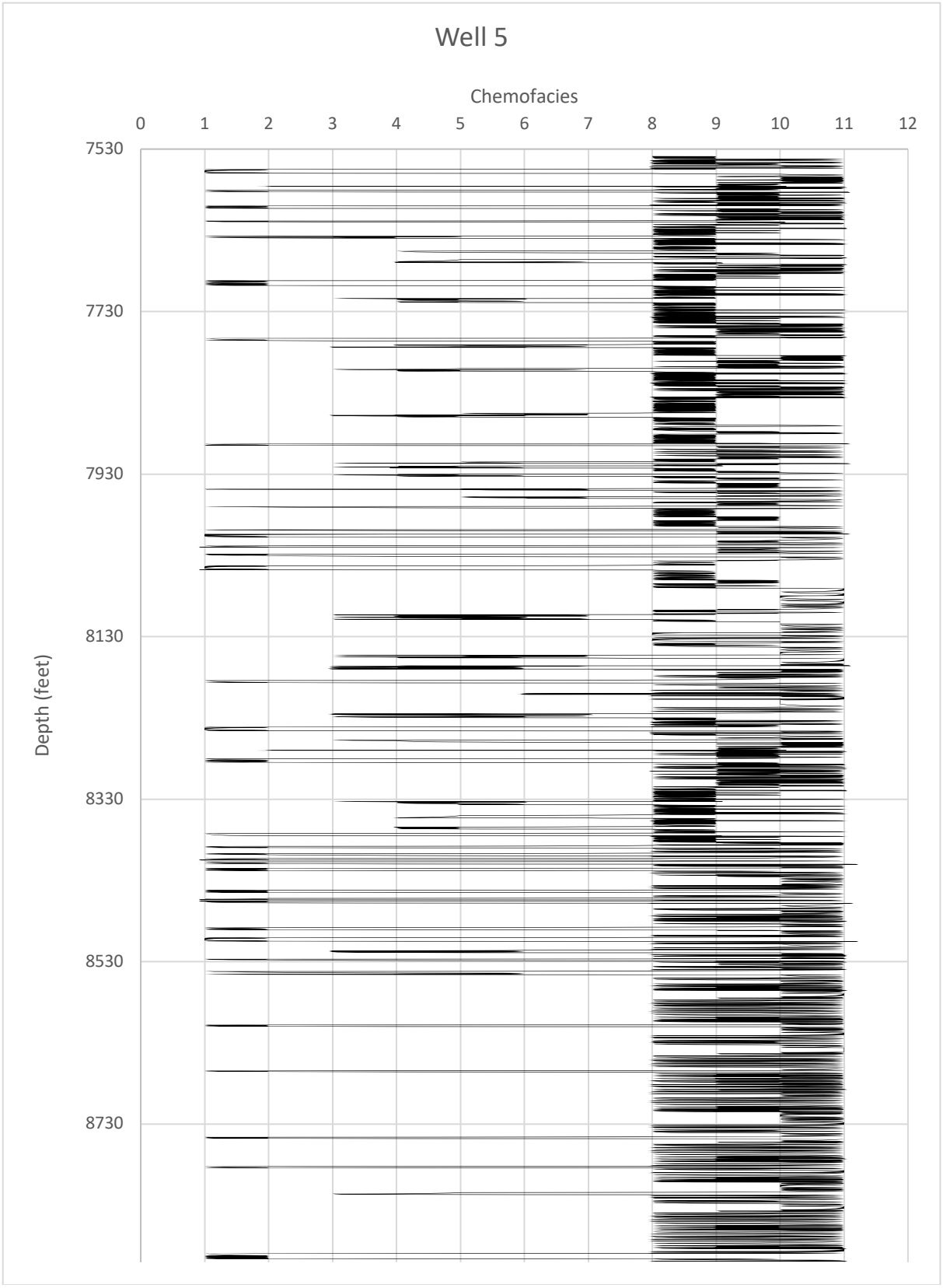
Well 5
Chemofacies
0
1
2
3
4
5
6
7
8
9
10
11
12
Depth (feet)
7530
7730
7930
8130
8330
8530
8730

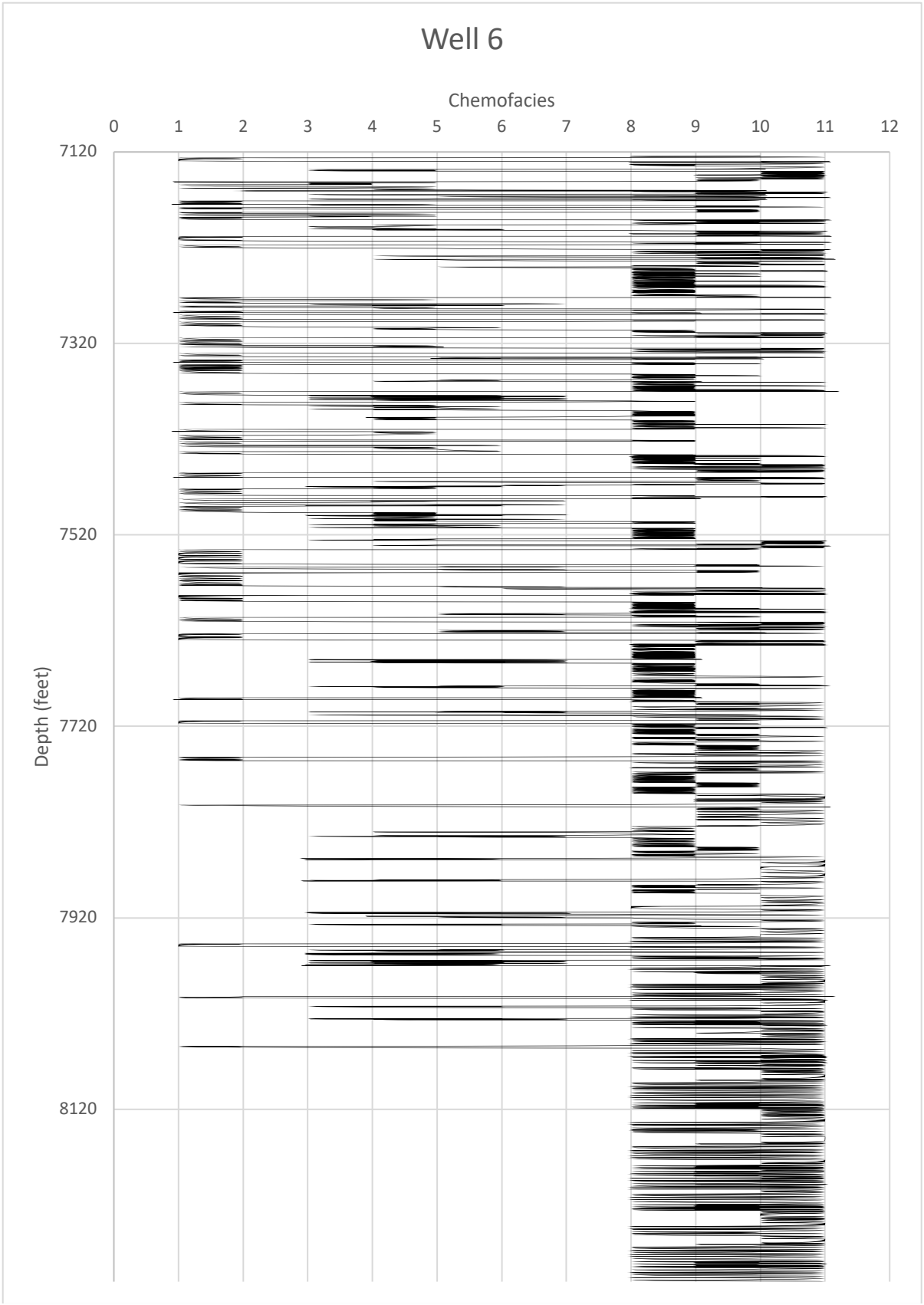
Well 6
Chemofacies
0
1
2
3
4
5
6
7
8
9
10
11
12
Depth (feet)
7120
7320
7520
7720
7920
8120

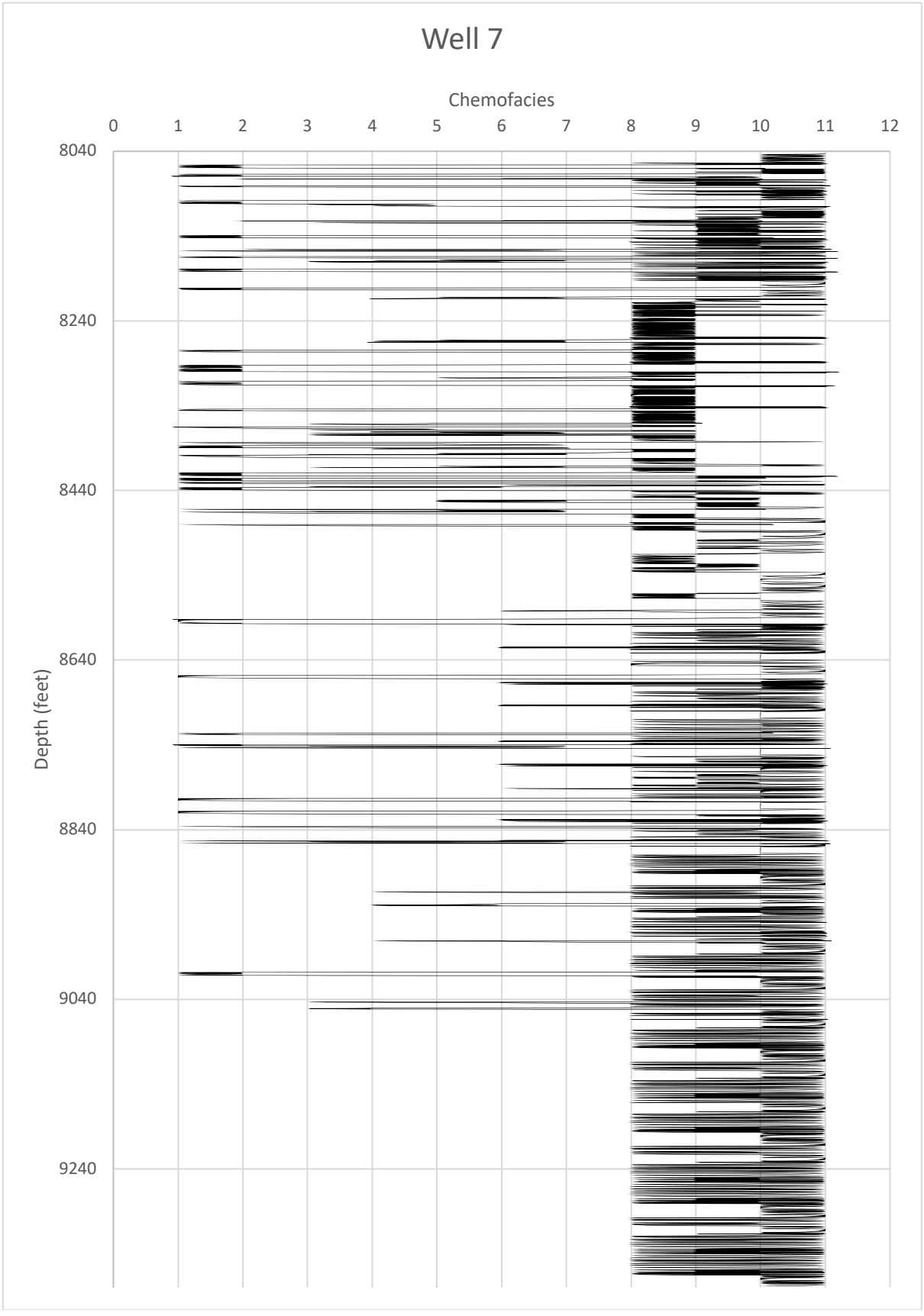
Well 7
Chemofacies
0
1
2
3
4
5
6
7
8
9
10
11
12
Depth (feet)
8040
8240
8440
8640
8840
9040
9240

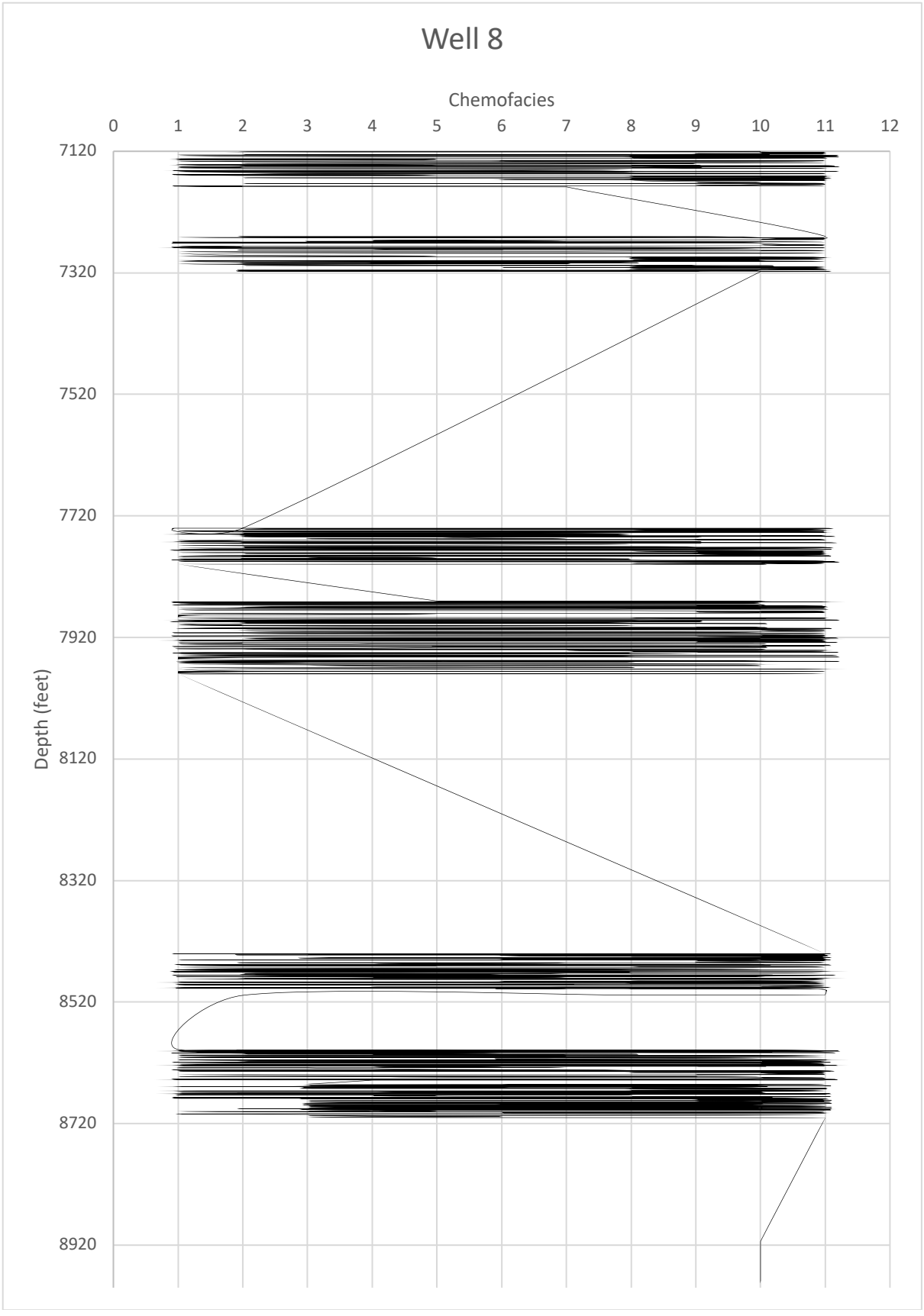
Well 8
Chemofacies
0
1
2
3
4
5
6
7
8
9
10
11
12
Depth (feet)
7120
7320
7520
7720
7920
8120
8320
8520
8720
8920

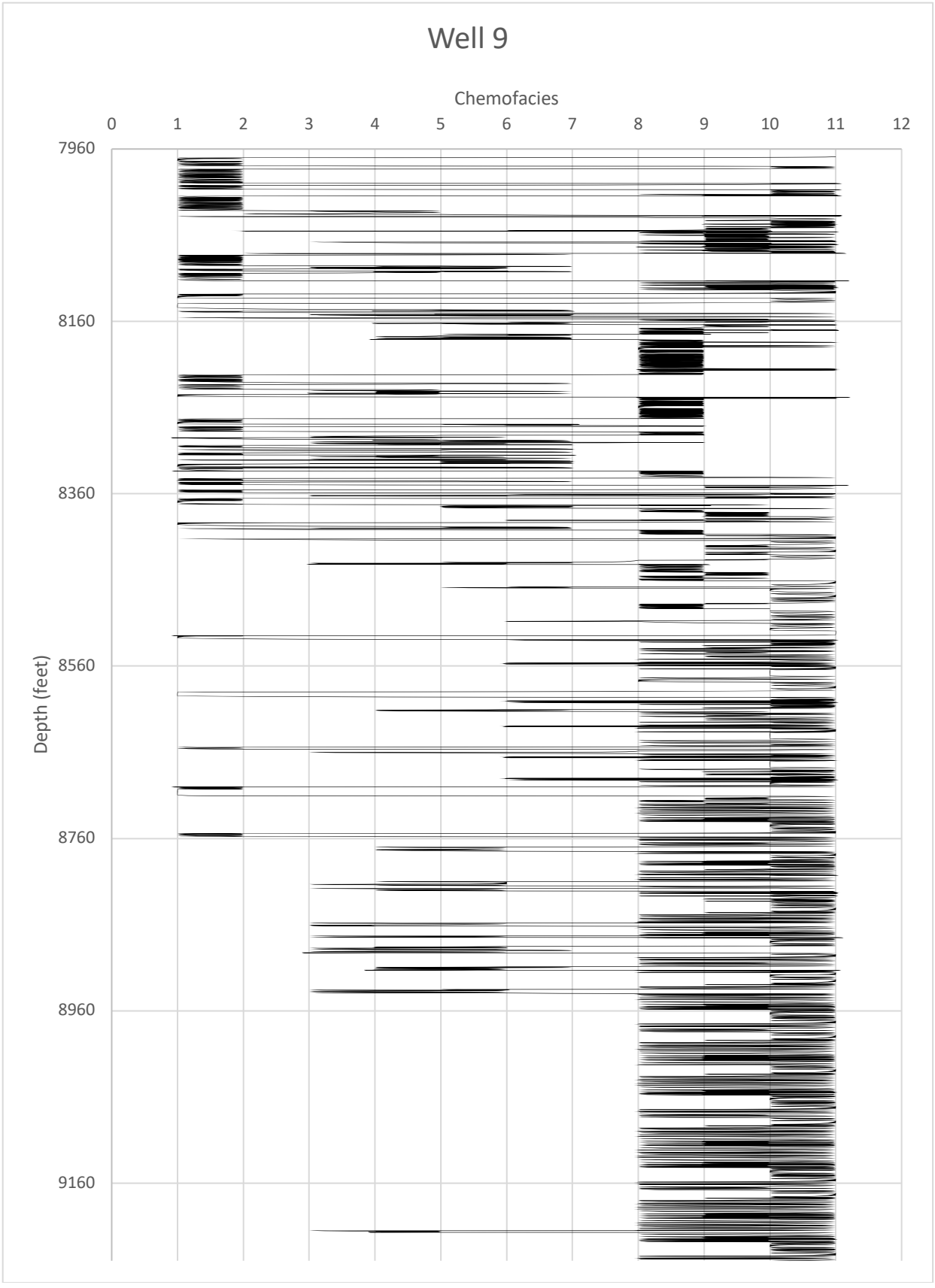
Well 9
Chemofacies
0
1
2
3
4
5
6
7
8
9
10
11
12
Depth (feet)
7960
8160
8360
8560
8760
8960
9160

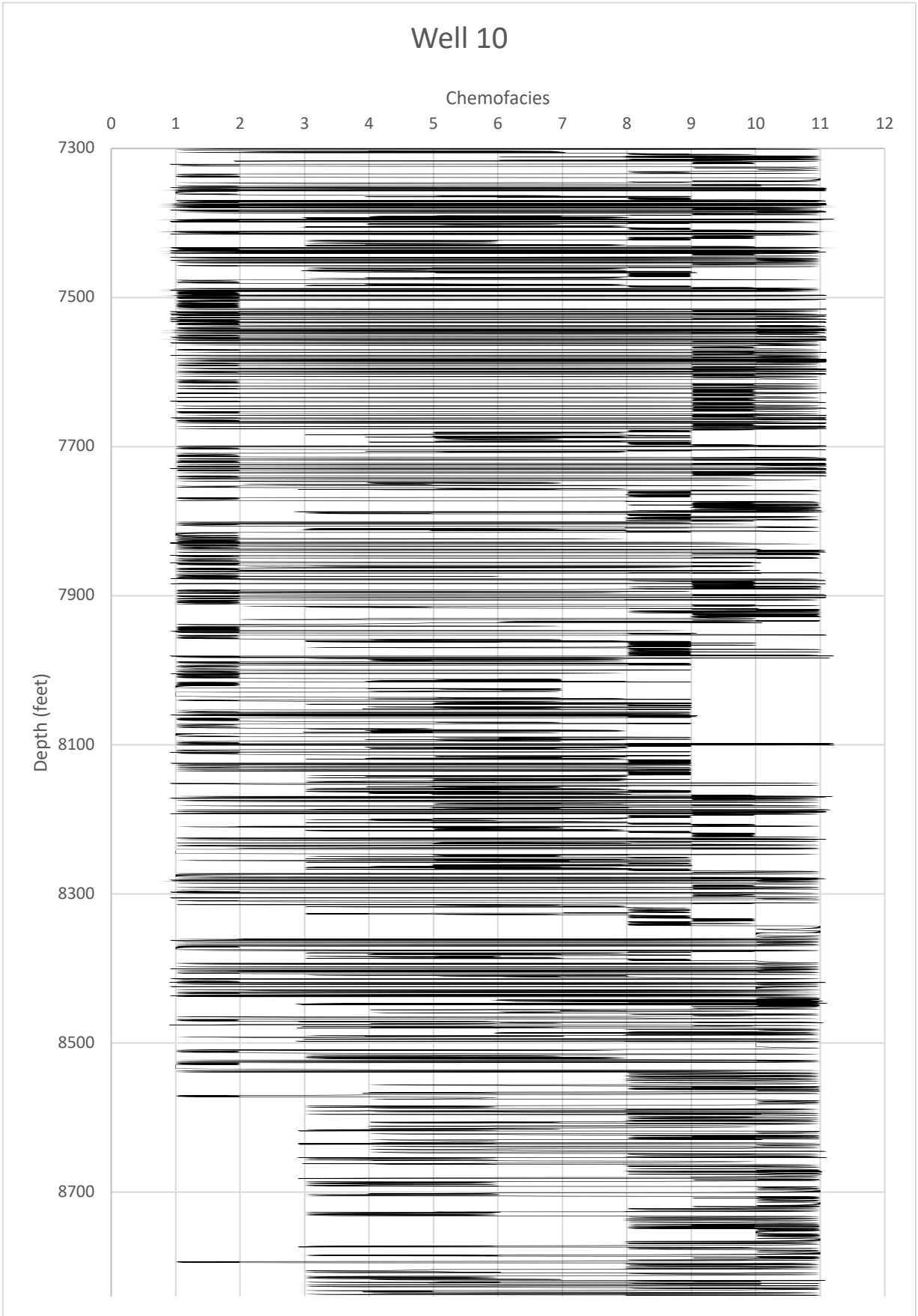
Well 10
Chemofacies
0
1
2
3
4
5
6
7
8
9
10
11
12
Depth (feet)
7300
7500
7700
7900
8100
8300
8500
8700

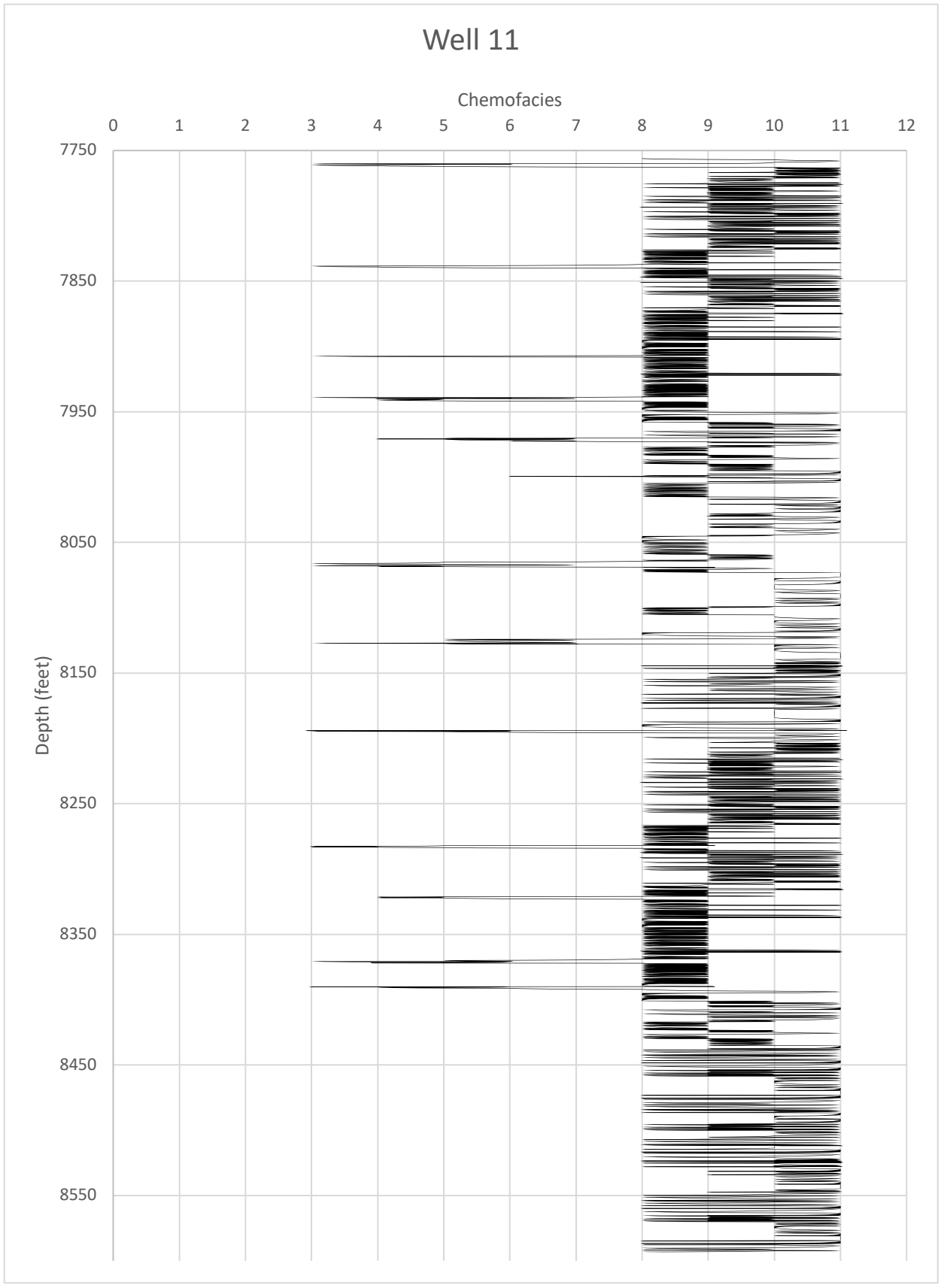
Well 11
Chemofacies
0
1
2
3
4
5
6
7
8
9
10
11
12
Depth (feet)
7750
7850
7950
8050
8150
8250
8350
8450
8550

REFERENCES

Adams, J. E., Frenzel, H. N., Rhodes, M. L., and Johnson, D. P., 1951, Starved Pennsylvanian Midland basin: AAPG Bulletin, v. 35, no. 12, p. 2600-2607.

Adams, J. E., and Rhodes, M. L., 1960, Dolomitization by seepage refluxion: AAPG bulletin, v. 44, no. 12, p. 1912-1920.

Ainsworth, R. B., and Pattison, S. A., 1994, Where have all the lowstands gone? Evidence for attached lowstand systems tracts in the Western Interior of North America: Geology, v. 22, no. 5, p. 415-418.

Baldwin, P. W., 2016, Lithostratigraphic and Geochemical Characterization of the Upper Pennsylvanian 'Wolfcamp D'Shale, Midland Basin (USA): Implications for Paleoenvironments and Unconventional Petroleum Reserviors.

Baumgardner, R., Hamlin, H., and Rowe, H., 2016, Lithofacies of the Wolfcamp and Lower Leonard intervals, southern Midland Basin: Texas: Austin, Texas, The University of Texas at Austin Bureau of Economic Geology Report of Investigations, v. 281, p. 66.

Baumgardner, R. W., and Rowe, H. D., 2017, PS Using Hierarchical Cluster Analysis to Improve Facies Definitions in Permian Mudrocks (Wolfcamp and Lower Leonard), Midland Basin, Texas: Geochemistry, v. 23, p. 2198-2213.

Bertram, G. T., 2012, Seismic and sequence stratigraphic analysis: Regional geology and tectonics: Principles of geologic analysis, v. 1, p. 864.

Bhatnagar, P., Scipione, M., Verma, S., and Bianco, R., 2018, Characterization of mass transport deposit using seismic attributes: Spraberry Formation, Midland Basin, West Texas, SEG Technical Program Expanded Abstracts 2018, Society of Exploration Geophysicists, p. 1618-1622.

Bhatnagar, P., Verma, S., and Bianco, R., 2019, Characterization of mass transport deposits using seismic attributes: Upper Leonard Formation, Permian Basin: Interpretation, v. 7, no. 4, p. SK19-SK32.

Blakey, R. C., 2013, Using paleogeographic maps to portray Phanerozoic geologic and paleotectonic history of western North America: AAPG Bulletin, v. 97, p. 146.

Blakey, R. C., and Fielding, C., 2008, Gondwana paleogeography from assembly to breakup—A 500 my odyssey: Geological Society of America Special Papers, v. 441, p. 1-28.

Candelaria, M., Entzminger, D., Behnken, F., Sarg, J., and Wilde, G., 1992, Wolfcampian sequence stratigraphy of eastern Central Basin platform, Texas: AAPG Bulletin (American Association of Petroleum Geologists);(United States), v. 76, no. CONF-9204139--.

Catuneanu, O., 2019, Model-independent sequence stratigraphy: Earth-science reviews, v. 188, p. 312-388.

Cawood, P. A., and Buchan, C., 2007, Linking accretionary orogenesis with supercontinent assembly: Earth-Science Reviews, v. 82, no. 3-4, p. 217-256.

Chaudhary, A. S., Ehlig-Economides, C., and Wattenbarger, R., Shale oil production performance from a stimulated reservoir volume, *in* Proceedings SPE Annual Technical Conference and Exhibition2011, OnePetro.

Cortez, M., III, 2012, Chemostratigraphy, paleoceanography, and sequence stratigraphy of the Pennsylvanian - Permian section in the Midland Basin of West Texas, with focus on the Wolfcamp formationM.S.]: The University of Texas at Arlington, 121 p.

Craigie, N., 2018, Principles of Elemental Chemstratigraphy, Cham, Switzerland, Springer International Publishing AG.

Crowell, J. C., 1978, Gondwanan glaciation, cyclothems, continental positioning, and climate change: American Journal of Science, v. 278, no. 10, p. 1345-1372.

-, 1999, Pre-Mesozoic ice ages: their bearing on understanding the climate system, Geological Society of America.

Davis, H. E., 1953, North-south cross section through Permian basin of West Texas, West Texas Geological Society.

Dembicki, H., 2016, Practical Petroleum Geochemistry for Exploration and Production, Elsevier Science.

Dutton, S. P., Kim, E. M., Broadhead, R. F., Raatz, W. D., Breton, C. L., Ruppel, S. C., and Kerans, C., 2005, Play analysis and leading-edge oil-reservoir development methods in the Permian basin: Increased recovery through advanced technologies: AAPG bulletin, v. 89, no. 5, p. 553-576.

Elias, S., and Alderton, D., 2020, Encyclopedia of Geology, Elsevier Science.

Engle, M. A., Reyes, F. R., Varonka, M. S., Orem, W. H., Ma, L., Ianno, A. J., Schell, T. M., Xu, P., and Carroll, K. C., 2016, Geochemistry of formation waters from the Wolfcamp and "Cline" shales: Insights into brine origin, reservoir connectivity, and fluid flow in the Permian Basin, USA: Chemical Geology, v. 425, p. 76-92.

Ewing, T. E., Christensen, H. V., and Geology, U. o. T. a. A. B. o. E., 2016, Texas Through Time: Lone Star Geology, Landscapes, and Resources, University of Texas at Austin Bureau of Economic Geology.

Fielding, C. R., Frank, T. D., and Isbell, J. L., 2008, The late Paleozoic ice age—A review of current understanding and synthesis of global climate patterns, Resolving the late Paleozoic ice age in time and space, Volume 441, Special Paper, p. 343-354.

Flamm, D. S., 2008, Wolfcampian development of the nose of the Eastern shelf of the midland basin, Glasscock, Sterling, and Reagan Counties, Texas, Brigham Young University.

Frakes, L. A., Francis, J. E., and Syktus, J. I., 1992, Climate Modes of the Phanerozoic, 286 p.:

Frenzel, H., Bloomer, R., Cline, R., Cys, J., Galley, J., Gibson, W., Hills, J., King, W., Seager, W., and Kottlowski, F., 1988, The Permian basin region: Sedimentary cover—North American craton: US: Boulder, Colorado, Geological Society of America, The Geology of North America, v. 2, p. 261-306.

Green, H., Šegvić, B., Zanoni, G., Omodeo-Salé, S., and Adatte, T., 2020, Evaluation of shale source rocks and clay mineral diagenesis in the permian basin, USA: Inferences on basin thermal maturity and source rock potential: Geosciences, v. 10, no. 10, p. 381.

Haldar, S. K., 2020, Introduction to mineralogy and petrology, Elsevier.

Hamlin, H. S., 2009, Ozona sandstone, Val Verde Basin, Texas: Synorogenic stratigraphy and depositional history in a Permian foredeep basin: AAPG bulletin, v. 93, no. 5, p. 573-594.

Hamlin, H. S., and Baumgardner, R. W., 2012, Wolfberry (Wolfcampian-Leonardian) deep-water depositional systems in the Midland Basin: Stratigraphy, lithofacies, reservoirs, and source rocks, Bureau of Economic Geology, University of Texas at Austin.

Hammon, H., Prather, T., Rowe, H., Mainali, P., Matheny, M., and Krumm, R., Geochemical, Mineralogical, and Lithological Linkages in a Thick, Early Permian, Siliciclastic Succession, Midland Basin, West Texas, USA, *in* Proceedings Unconventional Resources Technology Conference, Denver, Colorado, 22-24 July 20192019, Unconventional Resources Technology Conference (URTeC); Society of …, p. 3843-3851.

Handford, C. R., 1981, Sedimentology and genetic stratigraphy of Dean and Spraberry formations (Permian), Midland basin, Texas: AAPG bulletin, v. 65, no. 9, p. 1602-1616.

Haq, B. U., Hardenbol, J., and Vail, P. R., 1987, Chronology of fluctuating sea levels since the Triassic: Science, v. 235, no. 4793, p. 1156-1167.

Hemmesch, N. T., Harris, N. B., Mnich, C. A., and Selby, D., 2014, A sequence-stratigraphic framework for the upper Devonian Woodford Shale, Permian Basin, west Texas: AAPG Bulletin, v. 98, no. 1, p. 23-47.

Hillel, D., and Hatfield, J. L., 2005, Encyclopedia of Soils in the Environment, Elsevier Amsterdam.

Hoak, T., Sundberg, K., and Ortoleva, P., 1998, Overview of the structural geology and tectonics of the Central Basin Platform, Delaware Basin, and Midland Basin, West Texas and New Mexico: Science Applications International Corp., Germantown, MD (United States).

Hobson, J. P., Caldwell, C. D., and Toomey, D. F., 1985, Early Permian deep-water allochthonous limestone facies and reservoir, west Texas: AAPG bulletin, v. 69, no. 12, p. 2130-2147.

Holditch, S. A., 2003, The increasing role of unconventional reservoirs in the future of the oil and gas business: Journal of petroleum technology, v. 55, no. 11, p. 34-79.

Holterhoff, P., 2010, Sequence Stratigraphy and Depositional Systems of the Eastern Shelf Lower Permian, Central Texas: Examining the Tropical Record of Late Paleozoic Climate Change, Permian Basin Section Sepm.

Jones, T., and Matchus, E., 1984, East-West cross-section through Permian Basin of West Texas: West Texas Geological Society Special Publication.

Kinley, T. J., Cook, L. W., Breyer, J. A., Jarvie, D. M., and Busbey, A. B., 2008, Hydrocarbon potential of the Barnett Shale (Mississippian), Delaware Basin, west Texas and southeastern New Mexico: AAPG bulletin, v. 92, no. 8, p. 967-991.

Koppes, M., Hallet, B., Rignot, E., Mouginot, J., Wellner, J. S., and Boldt, K., 2015, Observed latitudinal variations in erosion as a function of glacier dynamics: Nature, v. 526, no. 7571, p. 100-103.

Kvale, E. P., Bowie, C. M., Flenthrope, C., Mace, C., Parrish, J. M., Price, B., Anderson, S., and DiMichele, W. A., 2020, Facies variability within a mixed carbonate–siliciclastic sea-floor fan (upper Wolfcamp Formation, Permian, Delaware Basin, New Mexico): AAPG Bulletin, v. 104, no. 3, p. 525-563.

Lawton, T. F., Blakey, R. C., Stockli, D. F., and Liu, L., 2021, Late Paleozoic (Late Mississippian–Middle Permian) sediment provenance and dispersal in western equatorial Pangea: Palaeogeography, Palaeoclimatology, Palaeoecology, v. 572, p. 110386.

Mazzullo, S., 1995, Permian Stratigraphy and Facies, Permian Basin (Texas—New Mexico) and Adjoining Areas in the Midcontinent United States, The Permian of Northern Pangea, Springer, p. 41-60.

Mazzullo, S., Hipke, W., Wiedemeir, T., Wingate, T., Gaylord, M., and Reid, A., 1989, Dynamic stratigraphy of the Tubb and Dean formations (Early Permian), northern Midland basin, Texas: West Texas Geological Society: Bulletin, v. 29, p. 5-11.

Mazzullo, S., and Reid, A., 1987, Basinal Lower Permian facies, Permian basin: Part II: Depositional setting and reservoir facies of Wolfcampian–lower Leonardian basinal carbonates: West Texas Geological Society Bulletin, v. 26, no. 8, p. 5-10.

McManus, J., Berelson, W. M., Severmann, S., Poulson, R. L., Hammond, D. E., Klinkhammer, G. P., and Holm, C., 2006, Molybdenum and uranium geochemistry in continental margin sediments: paleoproxy potential: Geochimica et Cosmochimica acta, v. 70, no. 18, p. 4643-4662.

Meyers, P. A., 1994, Preservation of elemental and isotopic source identification of sedimentary organic matter: Chemical geology, v. 114, no. 3-4, p. 289-302.

-, 1997, Organic geochemical proxies of paleoceanographic, paleolimnologic, and paleoclimatic processes: Organic geochemistry, v. 27, no. 5-6, p. 213-250.

Meyers, P. A., Bernasconi, S. M., and Yum, J.-G., 2009, 20 My of nitrogen fixation during deposition of mid-Cretaceous black shales on the Demerara Rise, equatorial Atlantic Ocean: Organic Geochemistry, v. 40, no. 2, p. 158-166.

Mitchum Jr, R., Vail, P. R., and Thompson III, S., 1977, Seismic stratigraphy and global changes of sea level: Part 2. The depositional sequence as a basic unit for stratigraphic analysis: Section 2. Application of seismic reflection configuration to stratigraphic interpretation.

Morgan, W. A., Clopine, W., Kokkoros, G., and Wiley, B., 1996, Sequence stratigraphic framework and exploration potential of lower Permian (Wolfcampian) gravity-flow deposits, eastern Midland Basin, Texas: American Association of Petroleum Geologists, Tulsa, OK (United States).

Moscardelli, L., and Wood, L., 2016, Morphometry of mass-transport deposits as a predictive tool: Bulletin, v. 128, no. 1-2, p. 47-80.

Nicot, J.-P., Darvari, R., Eichhubl, P., Scanlon, B. R., Elliott, B. A., Bryndzia, L. T., Gale, J. F., and Fall, A., 2020, Origin of low salinity, high volume produced waters in the Wolfcamp Shale (Permian), Delaware Basin, USA: Applied Geochemistry, v. 122, p. 104771.

Peng, J., Fu, Q., Larson, T. E., and Janson, X., 2021, Trace-elemental and petrographic constraints on the severity of hydrographic restriction in the silled Midland Basin during the late Paleozoic ice age: Bulletin, v. 133, no. 1-2, p. 57-73.

Petrash, D. A., Gueneli, N., Brocks, J. J., Méndez-Dot, J. A., Gonzalez-Arismendi, G., Poulton, S. W., and Konhauser, K. O., 2016, Black shale deposition and early diagenetic dolomite cementation during Oceanic Anoxic Event 1: The mid-Cretaceous Maracaibo Platform, northwestern South America: American Journal of Science, v. 316, no. 7, p. 669-711.

Phillips, N. D., 1991, Refined subsidence analysis as a means to constrain Late Cenozoic fault movement, Ventura Basin, California: University of Texas at Austin.

Posamentier, H. W., Martinsen, O. J., and Shipp, R., 2011, The character and genesis of submarine mass-transport deposits: insights from outcrop and 3D seismic data: Mass-transport deposits in deepwater settings. Tulsa: SEPM, Special Publication, v. 96, p. 7-38.

Principaud, M., Mulder, T., Gillet, H., and Borgomano, J., 2015, Large-scale carbonate submarine mass-wasting along the northwestern slope of the Great Bahama Bank (Bahamas): Morphology, architecture, and mechanisms: Sedimentary Geology, v. 317, p. 27-42.

Ross, C. A., 1986, Paleozoic evolution of southern margin of Permian basin: Geological Society of America Bulletin, v. 97, no. 5, p. 536-554.

Rowe, H., Hughes, N., and Robinson, K., 2012, The quantification and application of handheld energy-dispersive x-ray fluorescence (ED-XRF) in mudrock chemostratigraphy and geochemistry: Chemical Geology, v. 324, p. 122-131.

Rowe, H., Wang, X., Fan, B., Zhang, T., Ruppel, S. C., Milliken, K. L., Loucks, R., Shen, Y., Zhang, J., and Liang, Q., 2017, Chemostratigraphic insights into fluvio-lacustrine deposition, Yanchang Formation, Upper Triassic, Ordos Basin, China: Interpretation, v. 5, no. 2, p. SF149-SF165.

Scheffler, K., Hoernes, S., and Schwark, L., 2003, Global changes during Carboniferous–Permian glaciation of Gondwana: Linking polar and equatorial climate evolution by geochemical proxies: Geology, v. 31, no. 7, p. 605-608.

Shanmugam, G., 2018, Slides, slumps, debris flows, turbidity currents, and bottom currents: Implications.

Shanmugam, G., and Moiola, R., 1982, Eustatic control of turbidites and winnowed turbidites: Geology, v. 10, no. 5, p. 231-235.

Silver, B. A., and Todd, R. G., 1969, Permian cyclic strata, northern Midland and Delaware basins, west Texas and southeastern New Mexico: AAPG Bulletin, v. 53, no. 11, p. 2223-2251.

Sinclair, S. W., Crespo, L., Waite, L., Smith, K., and Leslie, C., Resource assessment in the northern Midland Basin: Detailed mapping of Late Pennsylvanian, Wolfcampian, and Early Leonardian margins and flooding surfaces using well logs and seismic data, *in* Proceedings SPE/AAPG/SEG Unconventional Resources Technology Conference2017, OnePetro.

Sivils, D., Examples of Wolfcampian debris flow deposits from the Eastern Shelf of the Midland Basin, Glasscock County, Texas, *in* Proceedings Wolfcampian of West Texas (Permian Basin, Sierra Diablo and Hueco Mountains) shelfal and periplatform carbonate reservoirs and outcrop analogs: Core workshop and field trip guidebook, Permian Basin Section, SEPM Publication2001, Volume 41, p. 4-1.

Sivils, D., and Stoudt, E., Basinal Wolfcampian carbonate debris flow, Midland Basin, Texas, *in* Proceedings Wolfcampian of West Texas (Permian Basin, Sierra Diablo and Hueco Mountains)—shelfal and periplatform carbonate reservoirs and outcrop analogs: Permian Basin Section SEPM Core Workshop and Field Trip Guidebook, Publication2001, p. 5-1.

Slatt, R. M., 2013, Stratigraphic Reservoir Characterization for Petroleum Geologists, Geophysicists, and Engineers, Elsevier Science.

Tabor, N. J., Montañez, I. P., Scotese, C. R., Poulsen, C. J., Mack, G. H., Fielding, C., Frank, T., and Isbell, J., 2008, Paleosol archives of environmental and climatic history in

paleotropical western Pangea during the latest Pennsylvanian through Early Permian: Resolving the late Paleozoic ice age in time and space, v. 441, p. 291-303.

Torsvik, T. H., and Cocks, L. R. M., 2013, Gondwana from top to base in space and time: Gondwana Research, v. 24, no. 3-4, p. 999-1030.

Vail, P. R., Mitchum Jr, R., and Thompson III, S., 1977, Seismic stratigraphy and global changes of sea level: Part 3. Relative changes of sea level from Coastal Onlap: section 2. Application of seismic reflection Configuration to Stratigrapic Interpretation.

Van Der Loop, M., 1990, AMACKER TIPPETT VVOLFCAMP FIELD UPTON COUNTY, TEXAS.

Van Wagoner, J., Reservoir facies distribution as controlled by sea-level change, *in* Proceedings SEPM Mid-Year meeting, Golden, CO.1985, p. 91-92.

Van Wagoner, J., Posamentier, H., Mitchum, R., Vail, P., Sarg, J., Loutit, T., and Hardenbol, J., 1988, An overview of the fundamentals of sequence stratigraphy and key definitions.

Veevers, J. t., and Powell, C. M., 1987, Late Paleozoic glacial episodes in Gondwanaland reflected in transgressive-regressive depositional sequences in Euramerica: Geological Society of America Bulletin, v. 98, no. 4, p. 475-487.

Verma, S., and Scipione, M., 2020, The early Paleozoic structures and its influence on the Permian strata, Midland Basin: Insights from multi-attribute seismic analysis: Journal of Natural Gas Science and Engineering, v. 82, p. 103521.

Vest Jr, E., 1970, Oil fields of Pennsylvanian-Permian horseshoe atoll, west Texas.

Vidas, H., and Hugman, B., 2008, ICF International. Availability, Economics, and Production Potential of North American Unconventional Natural Gas SuppliesPrepared for The INGAA Foundation: Inc. by: ICF International.

Wahlman, G. P., Tasker, D. R., Verwer, K., Playton, T., and Harris, P., 2013, Lower Permian (Wolfcampian) carbonate shelf-margin and slope facies, Central Basin platform and Hueco Mountains, Permian Basin, west Texas, USA: Deposits, architecture and controls of carbonate margin, slope, and basinal settings: SEPM Special Publication, v. 105.

Wilde, G., 1976, Wolfcamp series: Lexicon of Permian Stratigraphic Names of the Permian Basin of West Texas and Southeastern New Mexico. West Texas Geological Society Publication, no. 76-66, p. 327-331.

Wilson, R. D., Chitale, J., Huffman, K., Montgomery, P., and Prochnow, S. J., 2020, Evaluating the depositional environment, lithofacies variation, and diagenetic processes of the Wolfcamp B and lower Spraberry intervals in the Midland Basin: Implications for reservoir quality and distribution: AAPG Bulletin, v. 104, no. 6, p. 1287-1321.

Yang, K.-M., and Dorobek, S. L., 1995, The Permian Basin of west Texas and New Mexico: Tectonic history of a “composite” foreland basin and its effects on stratigraphic development: Stratigraphic evolution of foreland basins: SEPM Special Publication, v. 52, p. 149-174.

Zhang, J., and Slatt, R., 2019, The significance of karst unconformities on overlying resource shales: Lessons learned from the Devonian Woodford Formation applied to the Permian Wolfcamp Shale: Interpretation, v. 7, no. 4, p. SK33-SK43.

VITA

Helen Hammon was born in Houston, Texas. After completing high school at Memorial Senior High School, she entered the University of Texas and received her Bachelor's in Science in Geology in May 2018 from the Jackson School of Geology. She worked for Premier Oilfield Group in Houston Texas for a year following the completion of her bachelor's degree. And then continued on at Louisiana State University perusing a Master's in Science in Geology degree focusing on geochemistry, sequence stratigraphy, and paleoclimate until completion in May 2022.